HHS Public Access

Author manuscript

Glia. Author manuscript; available in PMC 2020 April 29.

Published in final edited form as:

Glia. 2019 October ; 67(10): 1958–1975. doi:10.1002/glia.23678.

Transcriptional regulation of homeostatic and disease-associated-microglial genes by IRF1, LXRβ and CEBPα

Tianwen Gao,
Department of Neurology, Emory University, Atlanta, GA, USA 30322

Janna Jernigan,
University of Georgia, Athens, GA, USA

Syed Ali Raza, MBBS,
Department of Neurology, Emory University, Atlanta, GA, USA 30322

Eric B Dammer, PhD,
Department of Biochemistry, Emory University, Atlanta, GA, USA 30322

Hailian Xiao,
Department of Neurology, Emory University, Atlanta, GA, USA 30322

Nicholas T Seyfried, PhD,
Department of Neurology, Emory University, Atlanta, GA, USA 30322

Allan I Levey, MD, PhD,
Department of Neurology, Emory University, Atlanta, GA, USA 30322

Srikant Rangaraju, MD, MS
Department of Neurology, Emory University, Atlanta, GA, USA 30322

Abstract

Microglia transform from homeostatic to disease-associated-microglia (DAM) profiles in neurodegeneration. Within DAM, we recently identified distinct pro-inflammatory and anti-inflammatory sub-profiles although the transcriptional regulators of homeostatic and distinct DAM gene profiles in microglia remain unclear. Informed by our previous studies, we nominated CEBPα, IRF1 and LXRβ as likely regulators of homeostatic, pro-inflammatory and anti-inflammatory DAM states and performed *in-vitro* siRNA studies in primary microglia to identify the role of each TF in regulating microglial activation, using an integrated transcriptomics, bioinformatics and experimental validation approach. Efficient (>70%) silencing of each TF in primary microglia revealed reciprocal regulation between each TF specifically following pro-

Corresponding author/Lead contact: Srikant Rangaraju, Srikant.rangaraju@emory.edu.

Authors' Contributions: Conceptualization: SR, TG; Methodology: SR, TG, JJ, EBD, SAR; Investigation: TG, JJ, SR, EBD, SAR, DD, PR, TG and HX; Writing-Original draft: SR, EBD, SAR; Writing-Review and Editing: TG, JJ, SR, EBD, NTS, AIL; Funding Acquisition: SR, AIL, NTS; Resources: AIL, NTS; Supervision: SR, AIL.

Conflicts of interest: The authors declare that they have no conflicts of interest.

Availability of data and material: Associated datasets are provided as supplemental files associated with this manuscript.

Consent for publication: All authors have approved of the contents of this manuscript and provided consent for publication.

Ethics approval and consent to participate: Approval from the Emory University Institutional Animal Care and Use Committee was obtained prior to all animal-related studies (IACUC protocol # 300123).

inflammatory activation. Neuroinflammatory transcriptomic profiling of microglia coupled with qPCR validation revealed distinct gene clusters with unique patterns of regulation by each TF which were independent of LPS stimulation. While all three TFs (especially IRF1 and LXRβ) positively regulated core DAM genes (Apoe, Axl, Clec7a, Tyrobp and Trem2) as well as homeostatic and pro-inflammatory DAM genes, LPS and IFNγ increased pro-inflammatory DAM but suppressed homeostatic and anti-inflammatory DAM gene expression via an Erk1/2-dependent signaling pathway. IRF1 and LXRβ silencing suppressed microglial phagocytic activity for macroparticles (polystyrene microspheres) as well as fAβ42 while IRF1 silencing strongly suppressed production of pro-inflammatory cytokines in response to LPS. Our studies reveal complex transcriptional regulation of homeostatic microglia and DAM profiles whereby IRF1, LXRβ and CEBPα positively regulate both pro- and anti-inflammatory DAM genes while activating stimuli independently augment pro-inflammatory DAM responses and suppress homeostatic and anti-inflammatory responses via Erk signaling. This framework can guide development of therapeutic immuno-modulatory strategies for neurodegeneration.

Keywords

microglia; transcriptional regulators; transcriptomics; phagocytosis; neuroinflammation; silencing RNA

INTRODUCTION

Microglia are the resident innate immune cells of the central nervous system (CNS) that constantly monitor their surrounding environment, prune neuronal synapses and are the “first responders” to an acute neurologic insult (Schafer et al. 2013, Crotti et al. 2016). Under activated conditions, microglia can perform pro-inflammatory roles as well as anti-inflammatory and protective functions including phagocytic clearance (Kreutzberg 1996, Saijo et al. 2013, Rangaraju et al. 2018). Transcriptomic profiling studies of the CNS from disease models have greatly advanced our knowledge of cellular diversity of the brain, especially heterogeneity within microglia (Gautier et al. 2012, Beutner et al. 2013, Hickman et al. 2013, Kim et al. 2013, Shay et al. 2013). Based on single cell RNAseq data, homeostatic microglia adopt distinct disease-associated-microglia (DAM) profiles in aging and chronic neurodegenerative diseases (Orre et al. 2014, Wang et al. 2015, Keren-Shaul et al. 2017). DAM also appears to be a heterogeneous group of cells and we recently identified distinct pro-inflammatory DAM and anti-inflammatory DAM subsets within DAM (Sarlus et al. 2017, Katkish et al. 2018). Flow cytometry studies confirmed that among $CD11c^+$ DAM, distinct $CD44^+$ and $CXCR4^+$ subsets exist, and pharmacologic studies demonstrated that these sub-profiles can be selectively modulated *in-vivo* (Katkish et al. 2018). Although signature genes highly expressed by these microglial states and transcriptional regulators of microglial development and survival (PU.1, MAFB, SALL1, IRF8) are now known (Kierdorf et al. 2013, Koshida et al. 2015, Buttgereit et al. 2016, Koso et al. 2016), the key upstream regulators of homeostatic, pro-inflammatory DAM and anti-inflammatory DAM transcriptional programs have not been identified.

In our recent network analysis of microglial transcriptomics data, we used pathway analyses to identify several TFs that may regulate homeostatic and distinct DAM phenotypes in the context of neurodegeneration (Katkish et al. 2018). However, confirmatory studies of regulatory roles for these putative TFs have not been performed. To address this knowledge gap, we first nominated the TFs with highest abundance in microglia and the most relevant TFs for homeostatic, pro-inflammatory DAM and anti-inflammatory DAM states (namely CEBPα, IRF1, and LXRβ). We performed *in-vitro* experiments by silencing each TF in primary mouse microglia under resting and activated states, followed by quantitative RT-PCR studies, neuroinflammatory transcriptomics (Nanostring) and inflammatory cytokine profiling. This approach allowed us to identify novel regulatory roles of TFs IRF1, LXRβ and CEBPα in regulating the expression of distinct clusters of genes as well as microglial states. Our studies also identified previously unknown cross-talk between each transcriptional pathway. Our results provide a transcriptional regulatory framework for microglial TFs IRF1, LXRβ and CEBPα that can guide future *in-vivo* studies and therapeutic immunomodulatory strategies for neurodegeneration.

MATERIALS AND METHODS

Primary neonatal microglia isolation:

Primary mouse microglial cultures were established using established isolation and enrichment protocols (Marek et al. 2008, Gordon et al. 2011). C57BL/6J mice (P0–3) were euthanized and brains were dissected then digested with Trypsin for 15 min at 37°C. After quenching the Trypsin with 20 ml DMEM (Dulbecco's Modified Eagle Medium)/10% fetal bovine serum (FBS) and 1% penicillin streptomycin glutamine, myelin debris were removed. The remaining cell suspension was filtered through a 40μm strainer and the cell pellet was washed followed by $CD11b^+$ positive selection using mini-MACS (Miltenyi Biotec Cat#130-042-201) column (Sarkar et al. 2017). $CD11b^+$ enrichment resulted in >90% pure $CD11b^+$ microglia as previously validated by flow cytometry (Gordon et al. 2011). Cells were then seeded in poly-L-lysine-coated wells and cultured in DMEM at 37°C incubator/5°C CO_2. After 24h, the medium was replaced with fresh medium, after which cells were ready for experimentation.

Small interfering RNA (siRNA) transfection studies:

Each TF was silenced using specific siRNA pools (IRF1 siRNA: sc-35707; LXRβ siRNA: sc-45317; CEBPα siRNA: sc-37048) or equal amounts of nonspecific sham siRNA (sc-37007) obtained from Santa Cruz biotechnology. Primary microglia were transfected with 40nM (final concentration) of siRNA using Lipofectamine™ RNAiMAX (Invitrogen) and Opti-MEM (Invitrogen, Cat #31985–062). Cells were cultured for 48h before to confirm the efficiency of siRNA-mediated gene silencing by quantitative reverse-transcriptase polymerase chain reaction (qRT-PCR). To activate microglia, lipopolysaccharide (LPS, final concentration 2ng/ml, #L4391, E. coli 0111:B4, Sigma-Aldrich) or recombinant mouse interferon γ (IFNγ #485-MI R&D Systems, final concentration 1–100ng/mL) was added after 24h of siRNA exposure and cells were collected after an additional 24h of activation for qRT-PCR, Nanostring and phagocytosis studies while supernatants were collected for cytokine assays.

Quantitative Nanostring neuroinflammatory gene expression and data analyses:

Microglia were exposed to siRNAs against IRF1, LXRβ and CEBPα for 24 h, followed by sham or LPS treatment (2ng/ml) for an additional 24 h after which cells were lysed in TRIzol (Invitrogen). RNA was then isolated using the nCounter low RNA input kit (Nanostring LOW-RNA-48). Quality control checks were performed on all samples to determine RNA concentration and integrity (RIN scores >7 for all samples). 100ng of RNA per sample was used for Nanostring studies. The Nanostring Neuroinflammation panel (770 selected genes) (Butovsky et al. 2014) was used for our experiments and samples were run in batches of 12 with appropriate randomization of all 24 samples to two batches. Gene expression was measured (Nanostring nCounter technology) and genes with counts above two-times the standard deviation of the negative control geomean were included in the final analysis. Of 770 genes, 662 genes met this criterion. The counts per gene were then normalized to the geometric mean of 8 housekeeping genes included in the panel. Principal component analysis (PCA) of the expression dataset was first performed to determine whether experimental conditions clustered together and to identify the most prominent experimental perturbation in the dataset. K-means cluster analysis was performed using Morpheus software (Broad Institute, https://software.broadinstitute.org/morpheus). T-distributed stochastic neighbor embedding (tSNE) was also performed on the Nanostring expression data as an orthogonal clustering approach (Broad Institute, https://software.broadinstitute.org/morpheus) and the agreement between K-means and tSNE clusters was determined by overlaying the two-dimensional tSNE scatter plot with K-means cluster membership (SPSS Version 24). Group-wise analysis of variance (ANOVA) followed by post-hoc Tukey's test was performed for comparisons across groups. Within each cluster, genes meeting group-wise ANOVA significance and post-hoc pairwise significance for the most deterministic treatment effect, were identified. Gene ontology (GO) analysis was performed to identify enriched GO terms, Wikipathways and KEGG pathways in within each cluster using all 662 included genes as the reference list (GOElite, Version 1.2.5) (Zambon et al. 2012).

Quantitative reverse transcriptase PCR (qRT-PCR)—RNA from microglia was extracted as previously described (Rangaraju et al. 2017). RNA concentration was assessed using Nanodrop and cDNA was synthesized using the high capacity cDNA reverse transcription kit (Applied Biosystems). Quantitative real-time PCR was performed on 7500 Fast Real-time PCR System (Applied Biosystems) using cDNA, TaqMan PCR Master Mix (Applied Biosystems), and gene-specific TaqMan probes (Applied Biosystems) against IRF1 (Mm01288580_m1), Nr1h2 (LXRβ) (Mm00437265_g1), Cebpa (CEBPα) (Mm00514283_s1), Spi (PU.1) (Mm00488140_m1), Il1β (Mm00434228_m1), Ptgs2 (Mm00478374_m1), Kcna3 (Mm00434599_s1), Apoe (Mm01307193_g1), Kcnj2 (Mm00434616_m1), Nceh1 (Mm00626772_m1), Timp2 (Mm00441825_m1), Tmem119 (Mm00525305_m1), P2ry12 (Mm01950543_s1), Tyrobp (Mm00449152_m1), Spp1 (Mm00436767_m1), Grn (Mm00433848_m1), C3ar1 (Mm02620006_s1), Lamp1 (Mm00495262_m1), Tnf (Mm01210732_g1), IL6 (Mm00443258_m1) and Gapdh (Mm99999915_g1). For each RNA sample, each primer set was run in duplicate. Relative gene expression analysis was performed using the 2-ΔΔCt method with the housekeeping gene GAPDH (Rangaraju et al. 2017). Primers for RT-qPCR were synthesized by Thermo-

Fisher Scientific. We also selectively inhibited Erk1/2 (SCH772984, 2uM), Jnk (SP600125, 2uM) and IKKβ/NFκB (IMD0354, 2uM) signaling pathways in microglia and determined the effects of pathway inhibition on gene expression of select microglial genes by qRT-PCR (Gafencu et al. 2007, Srinivasan et al. 2015).

Fluorescent Polystyrene Microsphere Phagocytosis Flow Cytometric Assay:

Phycoerythrin (PE)-conjugated polystyrene microspheres (Thermo-Fisher Fluorospheres, Cat #F13083) were added to primary microglia (Rangaraju et al. 2018). Cells were exposed to 5μl microspheres (microsphere to cell ratio approximately 200) for 1 hour followed by Trypsin incubation for 15 min at 37°C to detach the cells, after which DMEM with 10% fetal bovine serum was added and the cells were harvested by gentle pipetting on ice. Phagocytic characteristics were assayed by flow cytometry as previously described (Rangaraju et al. 2018). In this assay, distinct peaks of fluorescence are observed indicating unitary uptake of 1μm phycoerythrin polystyrene microspheres. All flow cytometric data were analyzed using FlowJo version 10 and proportions of cells demonstrating phagocytic uptake of >1 bead/cell were determined as an index of phagocytic activity.

Fluorescent Fibrillar Aβ42 Phagocytosis Assay:

Fibrillar fluorescent Aβ42 (conjugated to HiLyte Fluor 488) was prepared by mixing 100μg of peptide in 20μl 1% NH_4OH and immediately diluted with 1xPBS to 205.32μl to obtain 100μM final concentration. This was allowed to incubate at room temperature for 6 days and then used for phagocytosis assays as we have described previously (Rangaraju et al. 2018). After *in-vitro* exposure to siRNA and/or inflammatory stimuli, primary microglia were rinsed in the culture plate and then fAβ42–488 (2μM final concentration) was added for 1h at 37°C. Cells were then harvested as discussed above and then the washed cells were labeled with fluorophore-conjugated anti-CD45 mAb (CD45-PE-Cy7, BD Biosciences #552848). Compensation experiments were performed using compensation beads. Phagocytic uptake of fluorescent fAβ42 within live CD45+ microglia was measured as a proportion of fluorescent cells. We have already previously shown that this peak of fluorescence is inhibited by cytochalasin D treatment, confirming that our assay measures actin-dependent phagocytic processes (Rangaraju et al. 2018).

Multiplex immunoassays of cytokines and chemokines (Meso Scale Discovery platform V-PLEX):

Culture supernatants were collected prior to collection of cells for transcriptomic studies. Supernatants were centrifuged to remove debris and then 120μl was used for multiplex immunoassays (V-PLEX Proinflammatory panel: IFN-γ, IL-10, IL-12p70, IL-1β, IL-2, IL-4, IL-5, IL-6, KC/GRO, TNF-α), per manufacturer's instructions. These experiments were performed at the Emory Multiplexed Immunoassay Core (EMIC) and all samples were run in duplicate. Standard curves were created for each cytokine. Cytokine data were normalized to the overall mean and represented as a heat map (Morpheus software, Broad Institute). Group-wise ANOVA and post-hoc pairwise statistical comparisons were performed.

Human AD genome wide association study data:

To identify human AD-relevant genes that are regulated by each TF, we identified known human AD risk genes within each gene cluster that was identified in our Nanostring studies. We used a published list of 1,234 AD risk genes that were previously identified by Multi-marker Analysis of GenoMic Annotation (MAGMA) analysis of GWAS data from subjects with late-onset AD (Lambert et al. 2013, Seyfried et al. 2017, Rangaraju et al. 2018).

Statistical Analyses:

Graph-Pad version 7.0, Microsoft Excel version 2017, SPSS version 24 and R (version 3.5.1) were used for data analyses and data representation. Data from qRT-PCR studies of microglia are shown as mean ± standard error of mean (SEM). Student's T Test (two tailed, assuming equal variance) was used for pairwise comparisons, with statistical significance set at $p<0.05$ unless otherwise specified. All other statistical considerations are discussed in relevant sections above.

RESULTS

Selection of upstream transcriptional regulators of homeostatic and disease-associated-microglial (DAM) states

In a recent network-based analysis of microglial transcriptomic data, we identified gene co-expression modules that recapitulated homeostatic (annotated as Blue) and DAM profiles (Rangaraju et al. 2018) in agreement with single-cell RNAseq findings (Keren-Shaul et al. 2017); and identified distinct pro- and anti-inflammatory sub-profiles within DAM (annotated as Magenta and Yellow modules respectively; see Figure 1a) (Keren-Shaul et al. 2017, Katkish et al. 2018), each with distinct potential TF regulators (Supplemental Table S1, Figure 1b) (Katkish et al. 2018). To prioritize these potential TFs for experimental validation, we cross-referenced this list of TFs (Supplemental Table S1) with existing mouse microglial transcriptomic data (Zhang et al. 2014) to identify TFs for each microglial state with (a) highest probability of upstream regulation (enrichment Z-score), (b) high transcript abundance in microglia (abundance in microglia >50th percentile rank), and (c) microglial specificity (higher fold expression in microglia compared to other glial cells). Using this approach, we nominated one TF for each microglial state (Figure 1b): CEBPα for homeostatic microglia (enrichment Z score 4.6, 99th percentile abundance in microglia), IRF1 for pro-inflammatory DAM (Z score 11, 96th percentile abundance in microglia) and LXRβ for anti-inflammatory DAM (Z score 9.5, 96th percentile abundance in microglia) (Figure 1b). These TFs were then used for *in-vitro* experimental validation studies. In the case of TFs with closely related biology, such as IRF1 and IRF8 for pro-inflammatory DAM, and LXRα/LXRβ/RXR for anti-inflammatory DAM, we picked the TF that either lies upstream (IRF1 is upstream of IRF8) or the TF that was more abundantly expressed in microglia (LXRβ is more abundant in microglia compared to RXR and LXRα).

Silencing RNA-mediated suppression of IRF1, LXRβ and CEBPα in primary mouse microglia

To investigate the roles of TFs IRF1, LXRβ and CEBPα in regulating transcriptional states of microglia, we exposed primary mouse microglia to siRNAs against each TF in untreated microglia for 48h (Figure 1c). After 48h, we confirmed robust suppression of all three TFs by their respective siRNAs (Figure 2a), without any effects on microglial survival. After exposure to siRNAs for 24h, microglia were also stimulated with LPS (2ng/mL) for another 24h after which mRNA levels of each TF were measured. Again, we observed significant suppression of each target TF by the respective siRNA (Figure 2b). Under resting conditions, siRNA against either IRF1, LXRβ or CEBPα had no effect on the other TFs, suggesting their transcriptional independence from one another (Figure 2a). However, in LPS-stimulated microglia, we observed a significant divergence from this model. LPS upregulated IRF1 expression without affecting LXRβ and CEBPα expression. LXRβ siRNA reduced LPS-mediated IRF1 upregulation without affecting CEBPα. IRF1 siRNA suppressed both LXRβ and CEBPα expression. CEBPα siRNA suppressed LPS-mediated IRF1 upregulation and suppressed LXRβ expression. To summarize these findings, IRF1, LXRβ and CEBPα appear to be transcriptionally independent of each other in resting microglia (Figure 2c) but demonstrate bi-directional regulation of each other under pro-inflammatory activated states (Figure 2d), indicating cross-talk across distinct transcriptional pathways. Therefore, the effects of siRNA-mediated suppression of each of these TFs on microglial profiles needs to be considered both under resting as well as activated conditions.

Neuroinflammatory transcriptomic profiling of microglia identified distinct groups of genes regulated by IRF1, LXRβ and CEBPα

To comprehensively characterize regulation of microglial gene expression by IRF1, LXRβ and CEBPα, we performed Nanostring neuroinflammatory transcriptomic profiling (770 gene panel) of primary mouse microglia in response to siRNA against each TF in the presence or absence of LPS (Figure 3). Of 770 genes in the panel, 662 genes were expressed above noise in the 24-sample dataset (Supplemental Table S2). Principal component analysis (PCA) of the expression data revealed that regulation by IRF1 represented the most robust effect across the entire transcript panel (Figure 3a). We performed K-means clustering to identify groups of genes with similar co-expression patterns and identified 6 gene clusters of which clusters 1 to 5 demonstrated distinct patterns of gene expression (Figure 3b, Supplemental Table S2). Cluster 1 contained genes most strongly upregulated by LPS and positively regulated by IRF1 such as Ccl5, Cd69, Marco and Tnf. This cluster was enriched for gene ontology (GO) terms pertaining to biotic stimulus, immune activation and NFκB signaling as would be expected in response to LPS (Figure 4a, Supplemental Table S3). Cluster 2 contained genes (Tet1, Kif2x, Bok, Gja1) that were negatively regulated by IRF1 without alteration by LPS, and was enriched for GO terms related to nuclear localization, DNA metabolic process and chromosomal organization (Figure 4b). Cluster 3 represented a group of genes (Fcgr1, Gpr34, Cx3cr1, Fcrls, Apoe, Tyrobp, Csf1r) involved in phagocytosis, lysosomal biology, integrin response, TGFβ signaling and the Tyrobp causal network, that were down-regulated by LPS but positively regulated by IRF1 (Figure 4c). Cluster 4 was negatively regulated by all three TFs and contained genes related to neuronal dendrite biology, synaptic glutamatergic transmission and axonal projection, suggesting that

these microglial genes may be involved in synaptic pruning and microglia-neuronal interactions (Figure 4d). Cluster 5 represented a relatively small cluster of genes (Tbr1, Kcnj10, Ngo1, Csf1) which were negatively regulated by both LXRβ and IRF1, and enriched for Notch and mTOR signaling and the histone acetyltransferase complex (Figure 4e). A summary of regulation of each of the five gene clusters by IRF1, LXRβ and CEBPα is shown in Figure 4f (also see Supplemental Figure S1). We also validated IRF1-dependent positive regulation of several Cluster 3 and 1 genes which were picked based on high transcript abundance in microglia, neurodegenerative disease relevance and magnitude of effect observed in Nanostring studies (Tyrobp, Spp1, Grn, C3ar1 and Lamp1). Consistent with our Nanostring findings, we observed that IRF-1 positively-regulated these 5 genes under both resting and stimulated conditions, validating our Nanostring findings (Figure 3c).

Regulation of pro-inflammatory cytokine production and phagocytosis by IRF1, LXRβ and CEBPα

We next examined the effect of siRNAs against each of the TFs on inflammatory cytokine production in supernatants derived from the same experiments used for Nanostring studies (Figure 5a–b). Of 10 cytokines/chemokines in the MSD V-plex immunoassay, 7 factors were included in the final analysis while 3 factors were excluded due to values below the lowest detection thresholds. In unstimulated microglia, siRNAs against each TF did not alter cytokine production. Under LPS-activated conditions, IRF1 silencing strongly suppressed production of Tnf, IL12p70, KC/GRO, IL6, IL1b, IL5 and IL10. While siRNAs against LXRβ and CEBPα were partly effective in reducing LPS-induced cytokine production, siRNA against CEBPα more strongly suppressed production of IL6, IL1b and IL5. Interestingly, IL10 production induced by LPS was inhibited by siRNA against IRF1 and LXRβ but not CEBPα. Consistent with protein level changes, qRT-PCR studies also confirmed that Tnf and IL6 gene expression were also positively regulated by IRF-1 (Figure 5c). Overall, these multiplex immunoassays confirm that IRF1 had the strongest regulatory effect on pro-inflammatory cytokine production, followed by LXRβ and CEBPα in positively regulating pro-inflammatory cytokine production by microglia. These observations agree with our Nanostring results, where IRF1 suppression was observed to explain the largest proportion of variance in the dataset (Figure 3a). Since we also observed that the IRF1-dependent Cluster 3 contained AD-associated genes including Apoe, Tyrobp and others involved in phagocytic/endocytic processes, we determined whether silencing IRF1, LXRβ or CEBPα impacted the ability of microglia to phagocytose Aβ42 fibrils and polystyrene microspheres using a previously validated flow-cytometric assay (Rangaraju et al. 2018). In the fAβ42 phagocytosis assay, we observed increased phagocytic capacity in LPS-activated microglia and silencing each of the TFs inhibited the LPS-induced augmentation. However, all three TFs had no significant impact on the fAβ42 uptake under resting conditions (Figure 5e). In the PE-microsphere phagocytosis assay, we observed that IRF1 and LXRβ silencing inhibited phagocytic uptake (Figure 5e).

Regulation of homeostatic, pro-inflammatory DAM and anti-inflammatory DAM signature genes by IRF1, LXRβ and CEBPα

Next, we determined whether homeostatic and canonical DAM genes previously identified by single-cell RNAseq studies overlapped with clusters of genes regulated by IRF1, LXRβ

and CEBPα (Keren-Shaul et al. 2017). T-SNE was used to display transcriptomic data as distinct clusters in 2 dimensions and this approach showed excellent agreement with results from K-means clustering (Figure 6a). 73 homeostatic and 34 DAM genes were identified in our dataset (Supplemental Table S2). Among all clusters, cluster 3 was significantly enriched for both DAM and Homeostatic genes (Figure 6b, Chi Square statistic 52.2, $p<0.00001$) (Supplemental Figure S2) although no clear discernable pattern could be observed that distinguished DAM from homeostatic genes within the observed clusters. We also observed that core DAM genes (including Apoe, Clec7a, Tyrobp, Axl and Trem2) were all members of Cluster 3 (Supplemental Figure S3) (Keren-Shaul et al. 2017, Krasemann et al. 2017).

We also integrated our recent findings of distinct microglial co-expression modules (Rangaraju et al. 2018) with our transcriptomic results (Figure 6c). In this recent network meta-analysis of microglial transcriptomic data, we identified 20 co-expression modules including two homeostatic co-expression modules (Blue and Purple) and two DAM modules (Magenta: pro-inflammatory DAM, and Yellow: anti-inflammatory DAM) (Katkish et al. 2018). From the overall distribution of these microglial co-expression modules in our Nanostring expression data, (Figure 6c) we conclude that the Magenta pro-inflammatory DAM module is enriched in the LPS-upregulated and IRF1-dependent Cluster 1 while the anti-inflammatory DAM and homeostatic Blue modules were represented in clusters 2, 3 and 4. This suggests that partial segregation of pro- and anti-inflammatory DAM genes occurs with regards to upstream regulation by IRF1, LXRβ and CEBPα.

We also calculated a synthetic eigengene to represent the average expression of each previously identified microglial co-expression module defined as any of the top 20% of gene transcripts of each module (ranked by module membership or KME) that were also identified in this study's Nanostring transcript dataset and determined the effects of siRNA against each TF and LPS on these synthetic eigengenes. Six microglial co-expression gene modules were well represented in our dataset (at least 10 genes per module) (Figure 6d). Overall, we observed that IRF1 positively regulated all six microglial co-expression modules. LXRβ appeared to most strongly regulate the Magenta (pro-inflammatory DAM) and Blue (homeostatic) module while CEBPα had the strongest regulatory effect on Yellow (anti-inflammatory DAM), Magenta and Blue modules.

Regulation of human AD-risk genes by CEBPα, IRF1 and LXRβ

GWAS of late-onset AD has identified several gene polymorphisms associated with AD risk (Lambert et al. 2013, Seyfried et al. 2017). Of 1,234 known AD risk genes identified by MAGMA (Seyfried et al. 2017), 42 genes were present in our 662-gene expression dataset. Although the distribution of these AD-risk genes did not reveal any cluster-specific enrichment pattern, (Figure 7a), AD risk genes with the strongest MAGMA significance were identified in Cluster 3 (Apoe, Bin1, Ms4a4a, Mef2c, Cd33) (Figure 7b). As shown in Figure 4f, Cluster 3 is also positively regulated by IRF1, LXRβ and CEBPα and negatively regulated by LPS/IFNγ. Therefore, this analysis indicates that regulation of Cluster 3 genes by all three TFs may be relevant to immune mechanisms of AD pathology.

Validation studies of homeostatic and DAM gene regulation by CEBPα, IRF1 and LXRβ

Guided by findings from our transcriptomic studies described above, we performed validation studies in primary mouse microglia (Figure 8). QRT-PCR studies were performed to examine the effects of siRNA against TFs IRF1, LXRβ and CEBPα on expression of signature genes of each microglial transcriptional state (Homeostatic: Tmem119, Pro-inflammatory DAM: IL1β, Kcna3/Kv1.3, Ptgs2; anti-inflammatory DAM: Apoe, Kcnj2/Kir2.1, Nceh1, Timp2) in unstimulated microglia. In unstimulated microglia (Figure 7a–b), CEBPα suppression did not affect Tmem119 expression although we observed a robust upregulation of IL1β and down-regulation of Apoe and Kcnj2. IRF1 suppression down-regulated the expression of IL1β, Apoe, Kcnj2, Nceh1 as well as Tmem119. LXRβ suppression down-regulated IL1β, Apoe, Kcnj2 and Tmem119 and upregulated Ptgs2 expression. This observed pattern of microglial gene regulation by TFs (Figure 8b), like our transcriptomic data, did not entirely conform to the predicted model of a single TF for each of the three microglial transcriptomic states. Instead, it appears that IRF1 positively regulates all three module genes while CEBPα and LXRβ positively regulate homeostatic and anti-inflammatory DAM genes.

We next assessed effects of TF silencing on module-specific genes under LPS-stimulated conditions (Figure 8c–d). As expected, LPS induced pro-inflammatory IL1β and Ptgs2 expression and suppressed anti-inflammatory DAM genes Apoe, Kcnj2 and Nceh1 without impacting homeostatic Tmem119. IRF1 suppression nearly completely inhibited LPS-mediated upregulation of IL1β and Ptgs2, confirming a critical role of IRF1 in regulating pro-inflammatory microglial activation. LPS-mediated suppression of anti-inflammatory DAM genes Apoe, Kcnj2 and Nceh1 was further augmented by IRF1 suppression. This finding suggests that LPS stimulation of microglia activates a pathway that strongly inhibits anti-inflammatory DAM genes (master suppressor) which is independent of IRF1. Also, our results suggest that IRF1 may be a positive regulator of both pro-inflammatory DAM and anti-inflammatory DAM transcriptional genes. CEBPα suppression partially inhibited LPS-induced upregulation of IL1β and Ptgs2. LPS-mediated suppression of Apoe was also partly augmented although no effects of CEBPα suppression on other anti-inflammatory DAM or homeostatic genes were observed. LXRβ suppression also partially inhibited LPS-induced IL1β expression without significantly altering Ptgs2 expression while LPS-induced suppression of Apoe, Timp2 and Nceh1 were augmented (Figure 8c).

To further examine whether IRF1 and LXRβ positively regulate homeostatic and anti-inflammatory DAM genes, we performed experiments in primary microglia using a general activator of IRF1-mediated signaling (IFNγ) and an agonist of LXR/RXR activity (T0901317) (Figure 9a). IFNγ, across a wide dose range, strongly upregulated IL1β and suppressed Tmem119 and Apoe, resembling the effects of LPS in primary microglia, confirming its positive regulation of pro-inflammatory DAM genes. T0901317 significantly upregulated expression of Apoe without any effects on IL1β or Tmem119 at low or high concentrations, confirming LXRβ's role in regulating anti-inflammatory DAM gene expression. However, lack of effect on Tmem119 or IL1β implies that other LXRs (such as LXRα) may have opposing effects on pro-inflammatory DAM genes, although we did not further explore this possibility. Since we observed that IRF1 positively regulates LXRβ

expression in activated but not resting states, it is possible that pathways down-stream of IRF1 may promote anti-inflammatory DAM gene expression, although this pathway may be relatively less active compared to pathways that suppress anti-inflammatory DAM gene expression. Since IFNγ is not a selective agonist of IRF1, it is also possible that mechanisms independent of IRF1 are activated via IFNγ (and LPS).

Identification of signaling pathways implicated in LPS and IFNγ-mediated suppression of homeostatic and anti-inflammatory DAM genes

Our results suggest that pro-inflammatory activation of microglia by LPS or IFNγ increases IRF1 and upregulates pro-inflammatory DAM genes while strongly suppressing homeostatic and anti-inflammatory DAM genes. However, IRF1 (along with LXRβ and CEBPα) appears to positively regulate homeostatic and anti-inflammatory DAM genes as well. We also showed that IRF1 is required for LPS-mediated augmentation of pro-inflammatory DAM genes but does not appear to be required for the suppressive effect of LPS on homeostatic and anti-inflammatory DAM genes. Since LPS and IFNγ also engage distinct signaling pathways, we also found that silencing IRF-1 inhibited the IFNγ-induced pro-inflammatory DAM gene augmentation without impacting the suppressive effect of IFNγ on homeostatic and anti-inflammatory DAM genes suppression (Figure S4). These confirm that both LPS and IFNγ-mediated suppression of homeostatic and anti-inflammatory DAM genes may occur via IRF1-independent pathways. To confirm this, we silenced IRF1 and stimulated microglia with IFN Previous studies investigating Apoe downregulation by LPS suggested that ERK and JNK signaling converge on a TF called AP1 which suppresses Apoe gene expression (Gafencu et al. 2007), while NFκB signaling is involved in pro-inflammatory gene upregulation by activating stimuli such as IFNγ (Qi et al. 2013, Srinivasan et al. 2015). Therefore, we selectively inhibited Erk1/2 signaling (SCH772984), Jnk signaling (SP600125) and Nfκb signaling (IMD0354) in primary microglia under resting and activated conditions (IFNγ) and measured homeostatic (Tmem119 and P2ry12), anti-inflammatory DAM (Apoe and Timp2) and pro-inflammatory DAM (IL1b and Ptgs2) genes by qRT-PCR. Under resting conditions (Figure 9b), we found that Erk1/2 inhibition downregulated Tmem119 but upregulated P2ry12, upregulated Timp2 and downregulated Ptgs2 while Jnk and Nfκb inhibitors had no significant effects. Following activation by IFNγ (Figure 9c), we found that Erk1/2 inhibition decreased both pro-inflammatory gene expression, and partly reversed IFNγ suppression of anti-inflammatory DAM genes, although the effects on Tmem119 and P2ry12 homeostatic genes were discordant. Again, Jnk and Nfκb inhibitors had minimal effects on gene expression.

Reciprocal regulation between IRF1, LXRβ and CEBPα with the microglial master regulator PU.1

The microglial master regulator PU.1 (Spi1) is critical for microglial survival and has been recently identified as a potential regulator of DAM genes (Kierdorf et al. 2013, Smith et al. 2013). To explore regulatory relationships between IRF1, LXRβ and CEBPα with PU.1 (Figure 10a), we first examined whether silencing IRF1, LXRβ and CEBPα affects PU.1 expression. Under resting conditions, IRF1 siRNA significantly suppressed PU.1 expression while LXRβ and CEBPα siRNAs had minimal effects. Under LPS-stimulated conditions, we again observed suppression of PU.1 expression by IRF1 siRNA, and LXRβ siRNA also

moderately suppressed PU.1 gene expression. These indicate that IRF1, and to some extent LXRβ, positively regulate or maintain PU.1 expression. We next silenced PU.1 in primary microglia (Figure 10b) using siRNA and found that under homeostatic conditions, PU.1 silencing decreased IRF1 expression without affecting LXRβ and CEBPα expression. PU.1 suppression also downregulated expression of IL1β, in agreement with a previous study (Marecki et al. 2001). Interestingly, under activated conditions, PU.1 silencing did not alter homeostatic or DAM gene expression significantly. In summary, these results suggest that PU.1 is a positive regulator of IRF1 and IRF1 also positively regulates PU.1 expression.

A cohesive model of regulation of homeostatic and DAM genes by transcriptional factors IRF1, LXRβ and CEBPα and Erk1/2 signaling pathway

Based on our results derived by transcriptomic and functional profiling as well as targeted validation studies, we propose a model (Figure 11) in which TFs IRF1, LXRβ and CEBPα perform complex and overlapping upstream regulation of homeostatic, pro-inflammatory DAM and anti-inflammatory DAM genes, rather than a simplistic model where one TF represents the master regulator of the entire transcriptional program. According to this model, IRF1, LXRβ and CEBPα have shared gene targets with significant cross-regulation across each transcriptional pathway. Of these three TFs, IRF1 plays a critical role in regulating pro-inflammatory microglial activation including IL1β expression but also positively regulates anti-inflammatory DAM genes such as Apoe and the homeostatic gene Tmem119. Classical activating stimuli (LPS or IFNγ) strongly suppress homeostatic and anti-inflammatory DAM genes and this suppression appears to be mediated by Erk1/2 signaling and is independent of IRF1, LXRβ and CEBPα. Like IRF1, LXRβ also appears to positively regulate homeostatic, pro-inflammatory and anti-inflammatory DAM genes. CEBPα also appears to positively regulate pro-inflammatory and anti-inflammatory DAM genes under resting conditions although its effect on IL1β expression under LPS-activation is opposite to that of resting microglia, suggesting additional intermediary or co-regulatory pathways. In this model, the master myeloid TF PU.1 and IRF1 reciprocally and positively regulate each other.

DISCUSSION

Neuroinflammation, primarily mediated by microglia, is accepted to play causal roles, rather than simply bystander roles, in AD and other neurodegenerative disorders (Leyns et al. 2017, Liberman et al. 2018). Highly-consistent findings from bulk and single-cell transcriptomic studies of microglia have found that homeostatic microglia gradually adopt unique transcriptomic states reflecting distinct phenotypes referred to as neurodegeneration-associated or disease-associated-microglia (DAM) profiles (Keren-Shaul et al. 2017, Deczkowska et al. 2018, Katkish et al. 2018). The DAM profile represents a highly heterogeneous pool of microglia although they can be easily distinguished from homeostatic microglia by down-regulation of homeostatic genes (such as Tmem119) and upregulation of core DAM genes including Apoe, Trem2, Cst7 and Itgax (Cd11c) (Keren-Shaul et al. 2017, Krasemann et al. 2017, Deczkowska et al. 2018). A Trem2-Apoe-dependent immune checkpoint has also been identified to regulate the transition from homeostatic microglia to DAM (Krasemann et al. 2017). Based on gene expression patterns and accumulation of

DAM around Aβ plaques in AD mouse models, it has been proposed that DAM are generally pro-phagocytic and protective (Keren-Shaul et al. 2017), although our recent studies suggest that additional molecular and functional heterogeneity exists within DAM in the form of distinct pro-inflammatory and anti-inflammatory DAM sub-profiles (Katkish et al. 2018). While pro-inflammatory DAM highly express immune response genes such as IRF1, IL1b, Hif1a and Ptgs2 (Cox2), anti-inflammatory DAM highly express immunosuppressive, lipid-metabolism-related and phagocytic genes such as Apoe, Igf1, Itgax, Tyrobp, Clec7a, Lpl and Cst7 (Terwel et al. 2011, Orre et al. 2014, Krasemann et al. 2017, Katkish et al. 2018). Identifying the key upstream regulators of these distinct microglial states is important as it can guide target selection and therapeutic development for neurodegenerative disorders (Katkish et al. 2018, Rustenhoven et al. 2018).

In this study, we nominated CEBPα, LXRβ and IRF1 as predicted and microglia-abundant transcriptional regulators of homeostatic, pro-inflammatory DAM and anti-inflammatory DAM states. Up-regulation of IRF1 expression is associated with pro-inflammatory microglia activation (Das et al. 2015) and is critical for the expression of pro-inflammatory mediators including IL1b in reactive microglia (Masuda et al. 2015). CEBPα participates in the modulation of microglial anti-inflammatory state polarization (Yu et al. 2017). LXRβ has been reported to regulate immune responses in myeloid cells, and LXR activation can mitigate neuroinflammation and neurodegenerative pathology (Secor McVoy et al. 2015, Katkish et al. 2018). Notably, increasing LXRβ reduces Aβ burden in AD mouse models (Hu et al. 2013). Using a broad and relatively unbiased approach of transcriptomic profiling of microglia following selective genetic silencing of each TF under resting and activated conditions, we found that these three TFs positively regulate homeostatic as well as both DAM states, of which IRF1 appeared to have the strongest regulatory role. All three TFs (particularly IRF1 and LXRβ) in our study strongly positively regulated core DAM genes including Apoe, Axl, Clec7a, Tyrobp and Trem2, suggesting that the transition from homeostatic to DAM genes is likely to be collectively regulated by these TFs rather than a single master regulator (Keren-Shaul et al. 2017, Krasemann et al. 2017). This seems logical from a teleological sense because the homeostatic to DAM transition appears to be a universal theme across various chronic neuroinflammatory and neurodegenerative disease models as well as advanced aging (Chiu et al. 2013, Keren-Shaul et al. 2017, Mathys et al. 2017, Friedman et al. 2018), and such an important pathway is likely to have some redundancy in its regulation.

The observed overlap and redundancy in transcriptional regulation of homeostatic and DAM genes by the TFs in our studies aligns with recent studies that identified PU.1, a master regulator of myeloid cell and microglial development, as a regulator of DAM gene expression (Rustenhoven et al. 2018). It is also possible that PU.1 lies upstream of IRF1, LXRβ and CEBPα. Supporting this notion, Rustenhoven et. al. showed that PU.1 silencing by siRNA in microglia indeed resulted in reduction in CEBPβ (Rustenhoven et al. 2018) and PU.1 activation has been shown to relieve GATA-1-mediated suppression of CEBPα and CEBPβ (Burda et al. 2009). In our siRNA studies to examine the cross-talk between PU.1 and these three TFs, we found that PU.1 and IRF1 positively regulated each other and PU.1 positively regulates IL1b expression without altering anti-inflammatory DAM or homeostatic DAM gene expression. Therefore, our findings are consistent with previous

reports that suggest that PU.1 is an upstream master regulator that synergizes and augments IRF1 and CEBPα-mediated gene regulation (Marecki et al. 2001). We also observed that PU.1 expression was significantly impacted by IRF1 silencing, suggesting that IRF1, like PU.1, may also play critical transcriptional regulatory roles in the homeostatic to DAM transition, and may do so in part by impacting PU.1 expression.

Activating stimuli such as LPS and IFNγ in our studies upregulated pro-inflammatory DAM and suppressed homeostatic and anti-inflammatory DAM genes, consistent with prior results from co-expression analysis of microglial transcriptomics data (Katkish et al. 2018). While LPS increased IRF1 expression, we found that, surprisingly, IRF1 (as well as LXRβ and CEBPα) positively regulated anti-inflammatory DAM and homeostatic genes. This suggests that LPS-mediated suppression of homeostatic and anti-inflammatory DAM genes must be mediated via alternate pathways that are independent of IRF1, LXRβ and CEBPα. Based on our results, we suggest that LPS-induced Erk1/2 signaling may be involved in this suppressive effect of LPS on homeostatic and anti-inflammatory DAM genes. Under LPS-treated conditions, this Erk1/2-dependent pathway is likely to overcome positive regulation of homeostatic and anti-inflammatory DAM genes by IRF1, LXRβ and CEBPα, resulting in a net suppressive effect on homeostatic and anti-inflammatory DAM genes. Since LPS/IFNγ induced pro-inflammatory DAM genes and this upregulation was significantly inhibited by Erk1/2 inhibition, it is likely that activation of the Erk1/2 pathway by LPS or IFNγ represents a key mechanism by which pro-inflammatory stimuli upregulate pro-inflammatory DAM genes and suppress homeostatic and anti-inflammatory DAM genes, independent of IRF1, LXRβ and CEBPα. In the context of neurodegeneration, where upregulation of anti-inflammatory DAM and suppression of homeostatic genes are consistently observed, our findings support the model that activating stimuli unique to neurodegeneration can induce DAM by collectively activating IRF1, LXRβ and CEBPα pathways without activation of the Erk1/2 pathway.

Our finding regarding the role of the Erk1/2 pathway in independently promoting pro-inflammatory DAM while suppressing homeostatic and anti-inflammatory DAM in AD is congruent with existing findings regarding the detrimental effects of increased Erk1/2 activation in AD models as well as the observed increased Erk1/2 activation in human AD brain (Pei et al. 2002, Zhu et al. 2002, Liu et al. 2003). Furthermore, activation of the Erk pathway has been proposed as a detrimental neurodegenerative disease mechanism that is independent of Aβ pathology (Pei et al. 2002). Since the desired therapeutic response of ideal neuro-immunomodulatory therapies for neurodegeneration should include inhibition of pro-inflammatory DAM responses while sparing or augmenting anti-inflammatory DAM responses, our findings strongly support the rationale for inhibiting Erk1/2 activation as a therapeutic strategy to mitigate detrimental neuroinflammatory responses in AD. Since Erk1/2 is also involved in tau phosphorylation and non-microglial disease mechanisms (Pei et al. 2002, Zhao et al. 2002), inhibition of Erk can also have beneficial effects via non-immune pathways. Future *in-vivo* studies using selective Erk inhibitors with CNS bioavailability will address the translational potential of this strategy.

In addition to developing a model for the regulation of homeostatic and DAM genes, we also identified novel clusters of genes that are regulated by IRF1, LXRβ and CEBPα. We

identified a pro-inflammatory cluster, cluster 1, that contained genes that were LPS-upregulated and positively regulated by IRF1 while cluster 3 represented a large group of genes downregulated by LPS but also positively regulated by IRF1. The positive regulation of both LPS-upregulated and LPS-downregulated genes by IRF1 supports dual roles for IRF1 in regulating pro- as well as anti-inflammatory microglial responses. Two other gene clusters (clusters 3 and 4) also showed interesting gene ontologies. Cluster 4 was negatively regulated by all three TFs and was characterized by genes involved in synaptic transmission and neuronal synapto-dendritic function. Given the emerging role for microglia in pruning of neuronal synapses during development and in homeostatic states (Paolicelli et al. 2011, Schafer et al. 2013, Um 2017, Sominsky et al. 2018), and their detrimental effects by phagocytosing live neurons (phagoptosis) in disease conditions (Sierra et al. 2013, Brown et al. 2014), it is possible that this cluster reflects microglia-mediated synaptic pruning that is down-regulated by IRF1, LXRβ and CEBPα. Another gene cluster, cluster 3, contained several core DAM genes (Apoe, Clec7a, Trem2, Axl, Tyrobp), genes involved in the Tyrobp causal pathway of AD and involved in phagocytosis/endocytosis (Keren-Shaul et al. 2017, Krasemann et al. 2017). Silencing IRF1 and LXRβ resulted in suppression of phagocytic uptake of fAβ42 as well as macroparticles in microglia in our studies. Therefore, it is possible that TFs IRF1 and LXRβ (and CEBPα to a lesser extent) shift microglial functional states from homeostatic synaptic pruning to a state of increased phagocytic capacity and phagocytic clearance in AD, both of which are expected features of anti-inflammatory DAM.

A limitation of our studies is the *in-vitro* nature of our experiments, use of post-natal microglia in our studies. It has been well established that transcriptomic profiles of microglia change rapidly during isolation and *in-vitro* culture conditions. Several homeostatic genes that are highly expressed by microglia in the brain (such as P2ry12) are detected at very low levels in culture conditions(Hammond 2018), explaining our discordant findings between Tmem119 and P2ry12 gene expression. Pure microglial cultures remove microglia from the CNS environment, depriving them of several glial and neuronal-derived trophic factors that may be necessary for their maintenance in the brain. Unfortunately, an *in-vitro* microglial model system that is truly representative of microglia in the brain, is currently lacking although this could be partly overcome by organotypic slice cultures and organoid culture systems that incorporate microglia-like iPSC-derived cells (Abud et al. 2017, Pocock et al. 2018). As a result, our findings using mouse microglia in *in-vitro* settings need to be further evaluated using microglia derived from human iPSCs as well as assessed *in-vivo* using targeted conditional and inducible genetic strategies to suppress or over-express potential TFs specifically in microglia. Our studies focused on modulating TF gene expression rather than directly altering TF functional activity. Therefore, our studies do not address trans-repression of TFs, where protein-protein interactions between TFs that bind to similar regions in regulatory elements of genes can directly influence the function of the adjacent TF, leading to complex co-regulatory effects on gene programs (Ghisletti et al. 2007, Ghisletti et al. 2009). Whether such mechanisms are involved in fine tuning the immunological balance between pro-inflammatory and anti-inflammatory DAM gene expression in AD and neurodegeneration, remains to be explored.

CONCLUSIONS

In summary, we have identified IRF1, LXRβ and CEBPα as transcriptional factors that positively regulate DAM gene signatures independent of pro-inflammatory activating stimuli such as LPS or IFNγ. We also provide evidence for Erk1/2 as a key signaling pathway and potential disease mechanism that suppresses homeostatic and anti-inflammatory responses while increasing pro-inflammatory responses independent of IRF1, LXRβ and CEBPα. This complex transcriptional regulatory framework of homeostatic and DAM responses that may guide development of therapeutic immunomodulatory strategies for neurodegeneration.

Supplementary Material

Refer to Web version on PubMed Central for supplementary material.

Funding:

Work supported by Emory Alzheimer's Disease Research Center Grant P50 AG025688, American Brain Foundation (SR #28301), Alzheimer's Association (SR #37102), NINDS (K08-NS099474-1) and Emory Neuroscience NINDS Core facilities (P30 NS055077).

LIST OF ABBREVIATIONS

AD	Alzheimer's disease
LPS	Lipopolysaccharide
DAM	Disease-associated-microglia
IRF1	Interferon response factor 1
CEBPα	CCAAT/enhancer-binding protein alpha
LXRβ	Liver X Receptor beta
NFκB	nuclear factor kappa-light-chain-enhancer of activated B cells
Jnk	c-Jun N-terminal kinase
Erk 1/2	Extracellularly regulated kinases 1 and 2

REFERENCES

Abud EM, Ramirez RN, Martinez ES, Healy LM, Nguyen CHH, Newman SA, et al. (2017). "iPSC-Derived Human Microglia-like Cells to Study Neurological Diseases." Neuron 94(2): 278–293.e279. [PubMed: 28426964]

Beutner C, Linnartz-Gerlach B, Schmidt SV, Beyer M, Mallmann MR, Staratschek-Jox A, et al. (2013). "Unique transcriptome signature of mouse microglia." Glia 61(9): 1429–1442. [PubMed: 23832717]

Brown GC and Neher JJ (2014). "Microglial phagocytosis of live neurons." Nat Rev Neurosci 15(4): 209–216. [PubMed: 24646669]

Burda P, Curik N, Kokavec J, Basova P, Mikulenkova D, Skoultchi AI, et al. (2009). "PU.1 activation relieves GATA-1-mediated repression of Cebpa and Cbfb during leukemia differentiation." Mol Cancer Res 7(10): 1693–1703. [PubMed: 19825991]

Butovsky O, Jedrychowski MP, Moore CS, Cialic R, Lanser AJ, Gabriely G, et al. (2014). "Identification of a unique TGF-beta-dependent molecular and functional signature in microglia." Nat Neurosci 17(1): 131–143. [PubMed: 24316888]

Buttgereit A, Lelios I, Yu X, Vrohlings M, Krakoski NR, Gautier EL, et al. (2016). "Sall1 is a transcriptional regulator defining microglia identity and function." Nat Immunol 17(12): 1397–1406. [PubMed: 27776109]

Chiu IM, Morimoto ET, Goodarzi H, Liao JT, O'Keeffe S, Phatnani HP, et al. (2013). "A neurodegeneration-specific gene-expression signature of acutely isolated microglia from an amyotrophic lateral sclerosis mouse model." Cell Rep 4(2): 385–401. [PubMed: 23850290]

Crotti A and Ransohoff RM (2016). "Microglial Physiology and Pathophysiology: Insights from Genome-wide Transcriptional Profiling." Immunity 44(3): 505–515. [PubMed: 26982357]

Das A, Chai JC, Kim SH, Lee YS, Park KS, Jung KH, et al. (2015). "Transcriptome sequencing of microglial cells stimulated with TLR3 and TLR4 ligands." BMC Genomics 16: 517. [PubMed: 26159724]

Deczkowska A, Keren-Shaul H, Weiner A, Colonna M, Schwartz M and Amit I (2018). "Disease-Associated Microglia: A Universal Immune Sensor of Neurodegeneration." Cell 173(5): 1073–1081. [PubMed: 29775591]

Friedman BA, Srinivasan K, Ayalon G, Meilandt WJ, Lin H, Huntley MA, et al. (2018). "Diverse Brain Myeloid Expression Profiles Reveal Distinct Microglial Activation States and Aspects of Alzheimer's Disease Not Evident in Mouse Models." Cell Rep 22(3): 832–847. [PubMed: 29346778]

Gafencu AV, Robciuc MR, Fuior E, Zannis VI, Kardassis D and Simionescu M (2007). "Inflammatory signaling pathways regulating ApoE gene expression in macrophages." J Biol Chem 282(30): 21776–21785. [PubMed: 17553793]

Gautier EL, Shay T, Miller J, Greter M, Jakubzick C, Ivanov S, et al. (2012). "Gene-expression profiles and transcriptional regulatory pathways that underlie the identity and diversity of mouse tissue macrophages." Nat Immunol 13(11): 1118–1128. [PubMed: 23023392]

Ghisletti S, Huang W, Jepsen K, Benner C, Hardiman G, Rosenfeld MG, et al. (2009). "Cooperative NCoR/SMRT interactions establish a corepressor-based strategy for integration of inflammatory and anti-inflammatory signaling pathways." Genes Dev 23(6): 681–693. [PubMed: 19299558]

Ghisletti S, Huang W, Ogawa S, Pascual G, Lin ME, Willson TM, et al. (2007). "Parallel SUMOylation-dependent pathways mediate gene- and signal-specific transrepression by LXRs and PPARgamma." Mol Cell 25(1): 57–70. [PubMed: 17218271]

Gordon R, Hogan CE, Neal ML, Anantharam V, Kanthasamy AG and Kanthasamy A (2011). "A simple magnetic separation method for high-yield isolation of pure primary microglia." J Neurosci Methods 194(2): 287–296. [PubMed: 21074565]

Hammond TR (2018). "Complex cell-state changes revealed by single cell RNA sequencing of 76,149 microglia throughout the mouse lifespan and in the injured brain." bioRxiv: 1–22.

Hickman SE, Kingery ND, Ohsumi TK, Borowsky ML, Wang LC, Means TK, et al. (2013). "The microglial sensome revealed by direct RNA sequencing." Nat Neurosci 16(12): 1896–1905. [PubMed: 24162652]

Hu Y, Yang Y, Yu Y, Wen G, Shang N, Zhuang W, et al. (2013). "Synthesis and identification of new flavonoids targeting liver X receptor beta involved pathway as potential facilitators of Abeta clearance with reduced lipid accumulation." J Med Chem 56(15): 6033–6053. [PubMed: 23844653]

Katkish LA, Rangaraju S, Rector TS, Gravely AA, Johnson GJ, Klein MA, et al. (2018). "Incidence of unprovoked venous thromboembolic events in patients with chronic lymphocytic leukemia." Leuk Lymphoma 59(2): 509–511. [PubMed: 28651451]

Keren-Shaul H, Spinrad A, Weiner A, Matcovitch-Natan O, Dvir-Szternfeld R, Ulland TK, et al. (2017). "A Unique Microglia Type Associated with Restricting Development of Alzheimer's Disease." Cell 169(7): 1276–1290 e1217. [PubMed: 28602351]

Kierdorf K, Erny D, Goldmann T, Sander V, Schulz C, Perdiguero EG, et al. (2013). "Microglia emerge from erythromyeloid precursors via Pu.1- and Irf8-dependent pathways." Nat Neurosci 16(3): 273–280. [PubMed: 23334579]

Kim CC and Lanier LL (2013). “Beyond the transcriptome: completion of act one of the Immunological Genome Project.” Curr Opin Immunol 25(5): 593–597. [PubMed: 24168965]

Koshida R, Oishi H, Hamada M and Takahashi S (2015). “MafB antagonizes phenotypic alteration induced by GM-CSF in microglia.” Biochem Biophys Res Commun 463(1–2): 109–115. [PubMed: 25998393]

Koso H, Tsuhako A, Lai CY, Baba Y, Otsu M, Ueno K, et al. (2016). “Conditional rod photoreceptor ablation reveals Sall1 as a microglial marker and regulator of microglial morphology in the retina.” Glia 64(11): 2005–2024. [PubMed: 27459098]

Krasemann S, Madore C, Cialic R, Baufeld C, Calcagno N, El Fatimy R, et al. (2017). “The TREM2-APOE Pathway Drives the Transcriptional Phenotype of Dysfunctional Microglia in Neurodegenerative Diseases.” Immunity 47(3): 566–581 e569. [PubMed: 28930663]

Kreutzberg GW (1996). “Microglia: a sensor for pathological events in the CNS.” Trends Neurosci 19(8): 312–318. [PubMed: 8843599]

Lambert JC, Ibrahim-Verbaas CA, Harold D, Naj AC, Sims R, Bellenguez C, et al. (2013). “Meta-analysis of 74,046 individuals identifies 11 new susceptibility loci for Alzheimer’s disease.” Nat Genet 45(12): 1452–1458. [PubMed: 24162737]

Leyns CEG, Ulrich JD, Finn MB, Stewart FR, Koscal LJ, Remolina Serrano J, et al. (2017). “TREM2 deficiency attenuates neuroinflammation and protects against neurodegeneration in a mouse model of tauopathy.” Proc Natl Acad Sci U S A 114(43): 11524–11529. [PubMed: 29073081]

Liberman AC, Trias E, da Silva Chagas L, Trindade P, Dos Santos Pereira M, Refojo D, et al. (2018). “Neuroimmune and Inflammatory Signals in Complex Disorders of the Central Nervous System.” Neuroimmunomodulation: 1–25. [PubMed: 29788018]

Liu F, Su Y, Li B and Ni B (2003). “Regulation of amyloid precursor protein expression and secretion via activation of ERK1/2 by hepatocyte growth factor in HEK293 cells transfected with APP751.” Exp Cell Res 287(2): 387–396. [PubMed: 12837293]

Marecki S, Riendeau CJ, Liang MD and Fenton MJ (2001). “PU.1 and multiple IFN regulatory factor proteins synergize to mediate transcriptional activation of the human IL-1 beta gene.” J Immunol 166(11): 6829–6838. [PubMed: 11359842]

Marek R, Caruso M, Rostami A, Grinspan JB and Das Sarma J (2008). “Magnetic cell sorting: a fast and effective method of concurrent isolation of high purity viable astrocytes and microglia from neonatal mouse brain tissue.” J Neurosci Methods 175(1): 108–118. [PubMed: 18786564]

Masuda T, Iwamoto S, Mikuriya S, Tozaki-Saitoh H, Tamura T, Tsuda M, et al. (2015). “Transcription factor IRF1 is responsible for IRF8-mediated IL-1beta expression in reactive microglia.” J Pharmacol Sci 128(4): 216–220. [PubMed: 26318672]

Mathys H, Adaikkan C, Gao F, Young JZ, Manet E, Hemberg M, et al. (2017). “Temporal Tracking of Microglia Activation in Neurodegeneration at Single-Cell Resolution.” Cell Rep 21(2): 366–380. [PubMed: 29020624]

Orre M, Kamphuis W, Osborn LM, Jansen AHP, Kooijman L, Bossers K, et al. (2014). “Isolation of glia from Alzheimer’s mice reveals inflammation and dysfunction.” Neurobiol Aging 35(12): 2746–2760. [PubMed: 25002035]

Paolicelli RC, Bolasco G, Pagani F, Maggi L, Scianni M, Panzanelli P, et al. (2011). “Synaptic pruning by microglia is necessary for normal brain development.” Science 333(6048): 1456–1458. [PubMed: 21778362]

Pei JJ, Braak H, An WL, Winblad B, Cowburn RF, Iqbal K, et al. (2002). “Up-regulation of mitogen-activated protein kinases ERK1/2 and MEK1/2 is associated with the progression of neurofibrillary degeneration in Alzheimer’s disease.” Brain Res Mol Brain Res 109(1–2): 45–55. [PubMed: 12531514]

Pocock JM and Piers TM (2018). “Modelling microglial function with induced pluripotent stem cells: an update.” Nat Rev Neurosci 19(8): 445–452. [PubMed: 29977068]

Qi Y, Zou LB, Wang LH, Jin G, Pan JJ, Chi TY, et al. (2013). “Xanthoceraside inhibits pro-inflammatory cytokine expression in Abeta25–35/IFN-gamma-stimulated microglia through the TLR2 receptor, MyD88, nuclear factor-kappaB, and mitogen-activated protein kinase signaling pathways.” J Pharmacol Sci 122(4): 305–317. [PubMed: 23966052]

Rangaraju S, Dammer EB, Raza SA, Rathakrishnan P, Xiao H, Gao T, et al. (2018). “Identification and therapeutic modulation of a pro-inflammatory subset of disease-associated-microglia in Alzheimer’s disease.” Mol Neurodegener 13(1): 24. [PubMed: 29784049]

Rangaraju S, Raza SA, Li NX, Betarbet R, Dammer EB, Duong D, et al. (2018). “Differential Phagocytic Properties of CD45(low) Microglia and CD45(high) Brain Mononuclear Phagocytes-Activation and Age-Related Effects.” Front Immunol 9: 405. [PubMed: 29552013]

Rangaraju S, Raza SA, Pennati A, Deng Q, Dammer EB, Duong D, et al. (2017). “A systems pharmacology-based approach to identify novel Kv1.3 channel-dependent mechanisms in microglial activation.” J Neuroinflammation 14(1): 128. [PubMed: 28651603]

Rustenhoven J, Smith AM, Smyth LC, Jansson D, Scotter EL, Swanson MEV, et al. (2018). “PU.1 regulates Alzheimer’s disease-associated genes in primary human microglia.” Mol Neurodegener 13(1): 44. [PubMed: 30124174]

Saijo K, Crotti A and Glass CK (2013). “Regulation of microglia activation and deactivation by nuclear receptors.” Glia 61(1): 104–111. [PubMed: 22987512]

Sarkar S, Malovic E, Plante B, Zenitsky G, Jin H, Anantharam V, et al. (2017). “Rapid and Refined CD11b Magnetic Isolation of Primary Microglia with Enhanced Purity and Versatility.” J Vis Exp(122).

Sarlus H and Heneka MT (2017). “Microglia in Alzheimer’s disease.” J Clin Invest 127(9): 3240–3249. [PubMed: 28862638]

Schafer DP and Stevens B (2013). “Phagocytic glial cells: sculpting synaptic circuits in the developing nervous system.” Curr Opin Neurobiol 23(6): 1034–1040. [PubMed: 24157239]

Secor McVoy JR, Oughli HA and Oh U (2015). “Liver X receptor-dependent inhibition of microglial nitric oxide synthase 2.” J Neuroinflammation 12: 27. [PubMed: 25889344]

Seyfried NT, Dammer EB, Swarup V, Nandakumar D, Duong DM, Yin L, et al. (2017). “A Multi-network Approach Identifies Protein-Specific Co-expression in Asymptomatic and Symptomatic Alzheimer’s Disease.” Cell Syst 4(1): 60–72 e64. [PubMed: 27989508]

Shay T and Kang J (2013). “Immunological Genome Project and systems immunology.” Trends Immunol 34(12): 602–609. [PubMed: 23631936]

Sierra A, Abiega O, Shahraz A and Neumann H (2013). “Janus-faced microglia: beneficial and detrimental consequences of microglial phagocytosis.” Front Cell Neurosci 7: 6. [PubMed: 23386811]

Smith AM, Gibbons HM, Oldfield RL, Bergin PM, Mee EW, Faull RL, et al. (2013). “The transcription factor PU.1 is critical for viability and function of human brain microglia.” Glia 61(6): 929–942. [PubMed: 23483680]

Sominsky L, De Luca S and Spencer SJ (2018). “Microglia: Key players in neurodevelopment and neuronal plasticity.” Int J Biochem Cell Biol 94: 56–60. [PubMed: 29197626]

Srinivasan M and Lahiri DK (2015). “Significance of NF-kappaB as a pivotal therapeutic target in the neurodegenerative pathologies of Alzheimer’s disease and multiple sclerosis.” Expert Opin Ther Targets 19(4): 471–487. [PubMed: 25652642]

Terwel D, Steffensen KR, Verghese PB, Kummer MP, Gustafsson JA, Holtzman DM, et al. (2011). “Critical role of astroglial apolipoprotein E and liver X receptor-alpha expression for microglial Abeta phagocytosis.” J Neurosci 31(19): 7049–7059. [PubMed: 21562267]

Um JW (2017). “Roles of Glial Cells in Sculpting Inhibitory Synapses and Neural Circuits.” Front Mol Neurosci 10: 381. [PubMed: 29180953]

Wang Y, Cella M, Mallinson K, Ulrich JD, Young KL, Robinette ML, et al. (2015). “TREM2 lipid sensing sustains the microglial response in an Alzheimer’s disease model.” Cell 160(6): 1061–1071. [PubMed: 25728668]

Yu A, Zhang T, Duan H, Pan Y, Zhang X, Yang G, et al. (2017). “MiR-124 contributes to M2 polarization of microglia and confers brain inflammatory protection via the C/EBP-alpha pathway in intracerebral hemorrhage.” Immunol Lett 182: 1–11. [PubMed: 28025043]

Zambon AC, Gaj S, Ho I, Hanspers K, Vranizan K, Evelo CT, et al. (2012). “GO-Elite: a flexible solution for pathway and ontology over-representation.” Bioinformatics 28(16): 2209–2210. [PubMed: 22743224]

Zhang Y, Chen K, Sloan SA, Bennett ML, Scholze AR, O'Keeffe S, et al. (2014). "An RNA-sequencing transcriptome and splicing database of glia, neurons, and vascular cells of the cerebral cortex." J Neurosci 34(36): 11929–11947. [PubMed: 25186741]

Zhao WQ, Ravindranath L, Mohamed AS, Zohar O, Chen GH, Lyketsos CG, et al. (2002). "MAP kinase signaling cascade dysfunction specific to Alzheimer's disease in fibroblasts." Neurobiol Dis 11(1): 166–183. [PubMed: 12460556]

Zhu X, Lee HG, Raina AK, Perry G and Smith MA (2002). "The role of mitogen-activated protein kinase pathways in Alzheimer's disease." Neurosignals 11(5): 270–281. [PubMed: 12566928]

MAIN POINTS

We identify a framework for homeostatic and disease-associated microglia (DAM) gene regulation. IRF1, LXRβ and CEBPα increase pro- and anti-inflammatory DAM genes while Erk1/2 signaling suppresses homeostatic and anti-inflammatory DAM while increasing pro-inflammatory DAM.

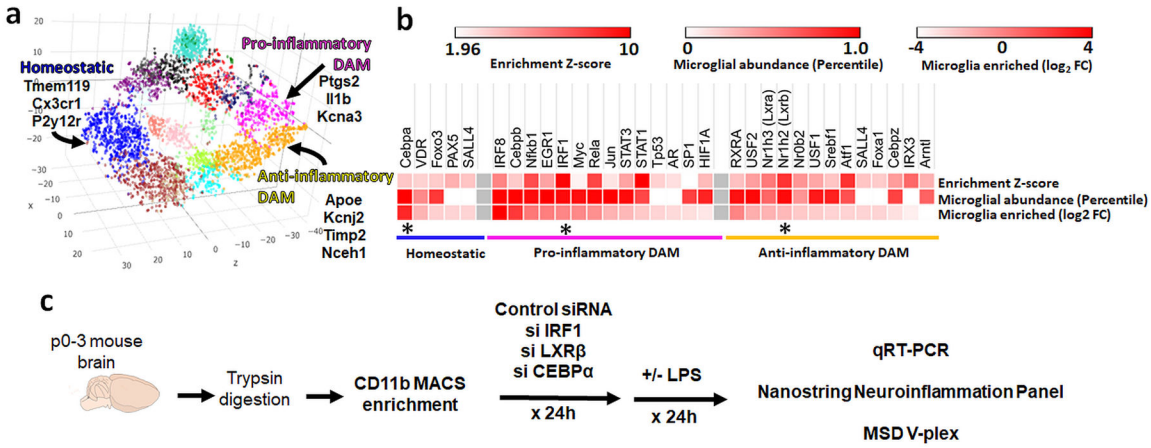

Figure 1. Nomination of TFs as regulators of homeostatic, pro-inflammatory DAM and anti-inflammatory DAM genes in microglia.

(a) A transcriptomic framework of microglial activation in AD that was identified by co-expression network analysis of microglial transcriptomes (Rangaraju et al. 2018). Each dot represents a single gene. Clusters of genes (co-expression modules) are color coded. Blue: Homeostatic gene cluster; Magenta: Pro-inflammatory DAM cluster; Yellow: Anti-inflammatory DAM cluster. Key genes within each cluster are shown.

(b) Heat map representation of enrichment Z-score for each predicted TF (grey scale), microglia abundance (based on RNAseq expression data from purified mouse microglia) and microglial specificity (Fold-enrichment in microglia as compared to other non-microglial cell types). Asterisks indicate the TFs selected for each microglial state using this approach.

(c) Experimental work flow for siRNA studies using primary p0–3 mouse microglia: Brains were digested by Trypsin followed by $CD11b^{+}$ column enrichment. Cultured microglia were treated with siRNAs for 24h followed by LPS (2ng/mL) or other activators for an additional 24h. Microglia and supernatants were then collected for Nanostring or qRT-PCR and for multiplex cytokine/chemokine immunoassays respectively.

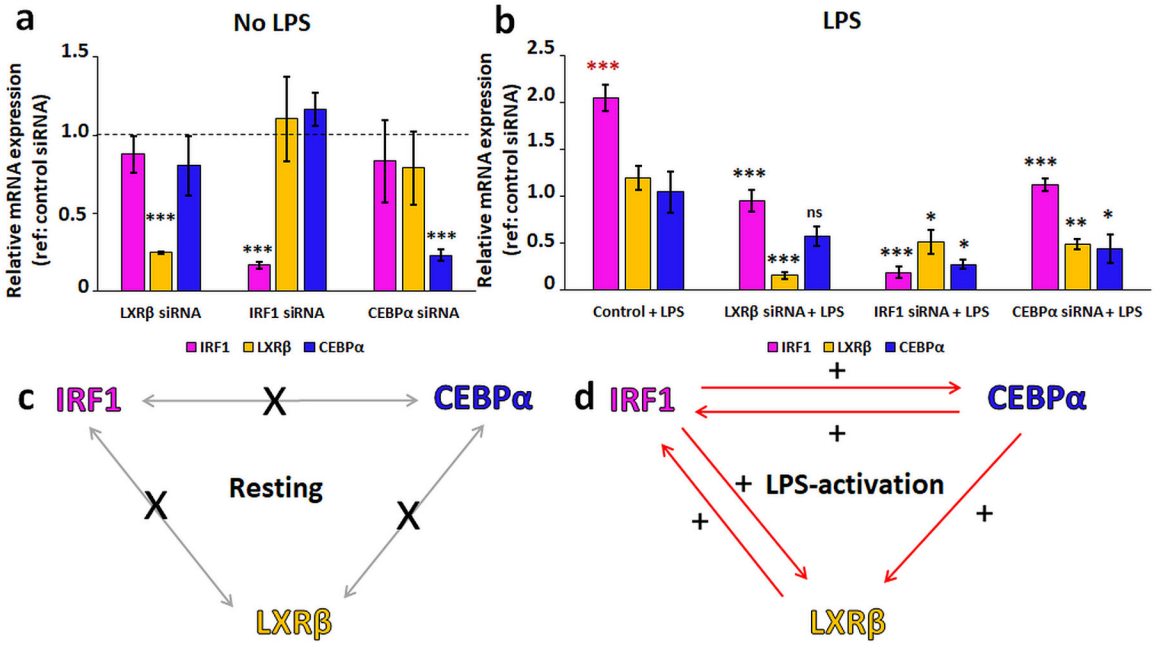

Figure 2. Silencing RNA-mediated suppression of TFs in primary microglia reveals activation state-dependent reciprocal cross talk.

(a) Results from qRT-PCR experiments demonstrating efficiency of TF silencing by each siRNA as compared to control siRNA. Y-axis represents relative mRNA expression (2-ΔΔCt method) normalized to Gapdh as housekeeping gene (3 independent biological replicate experiments were performed per condition, *P<0.05, **P<0.01, ***P<0.005).

(b) Results from qRT-PCR experiments confirming siRNA efficiency under LPS-activated conditions. Error bars represent standard error of mean. (3 independent biological replicate experiments were performed per condition; *P<0.05, **P<0.01, ***P<0.005).

(c, d) Summary of qRT-PCR studies highlighting relationships between the three TFs under resting (c) and LPS-activated (d) conditions. Red arrows indicate positive regulation while Blue arrows indicate negative regulation.

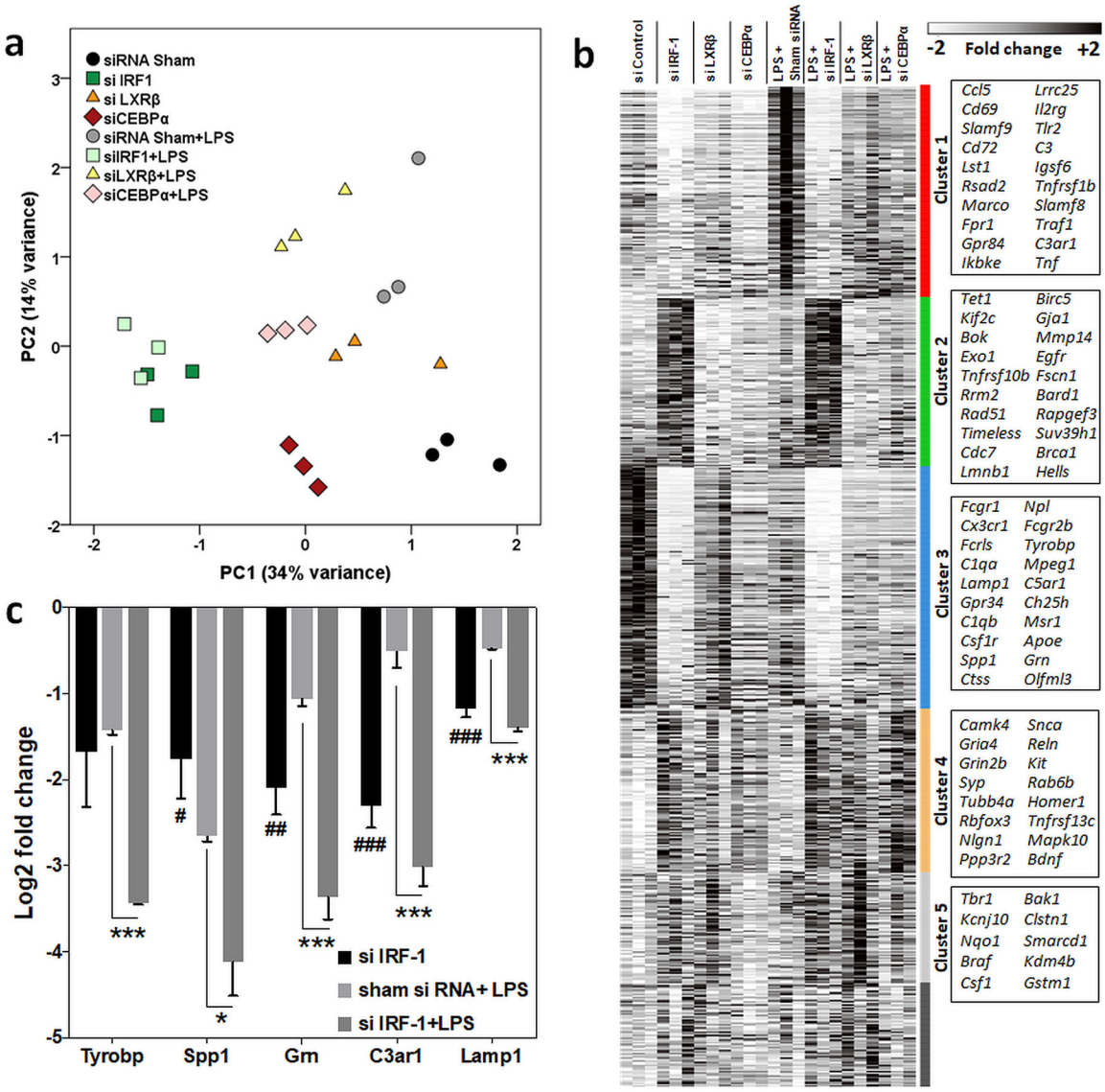

Figure 3. Transcriptomic profiling reveals distinct clusters of genes regulated by IRF1, LXRβ and CEBPα.

(a) Principal component analysis of Nanostring expression data (662 genes) demonstrating separation between each experimental condition. PC1 explained 34% while PC2 explained 14% of variance in the dataset. PC1 represents genes most strongly regulated by IRF1 while PC2 is representative of the LPS effect.

(b) Heat map representing results from K-means clustering analysis of Nanostring gene expression data. Cluster 1 genes: upregulated by LPS and positively regulated by IRF1; Cluster 2 genes: negatively regulated by IRF1 under resting and activated conditions; Cluster 3 genes: down-regulated by LPS, positively regulated by IRF1; Cluster 4 genes: negatively regulated by all three TFs; Cluster 5 genes: down-regulated by IRF1 and LXRβ.

(c) qRT-PCR validation of selected genes (Tyrobp, Spp1, Grn, C3ar1 and Lamp1) in IRF-1 siRNA treated microglia under resting and LPS-activated conditions (n=3 independent

biological replicates, error bars represent standard error of mean, *P<0.05, **P<0.01, ***P<0.005).

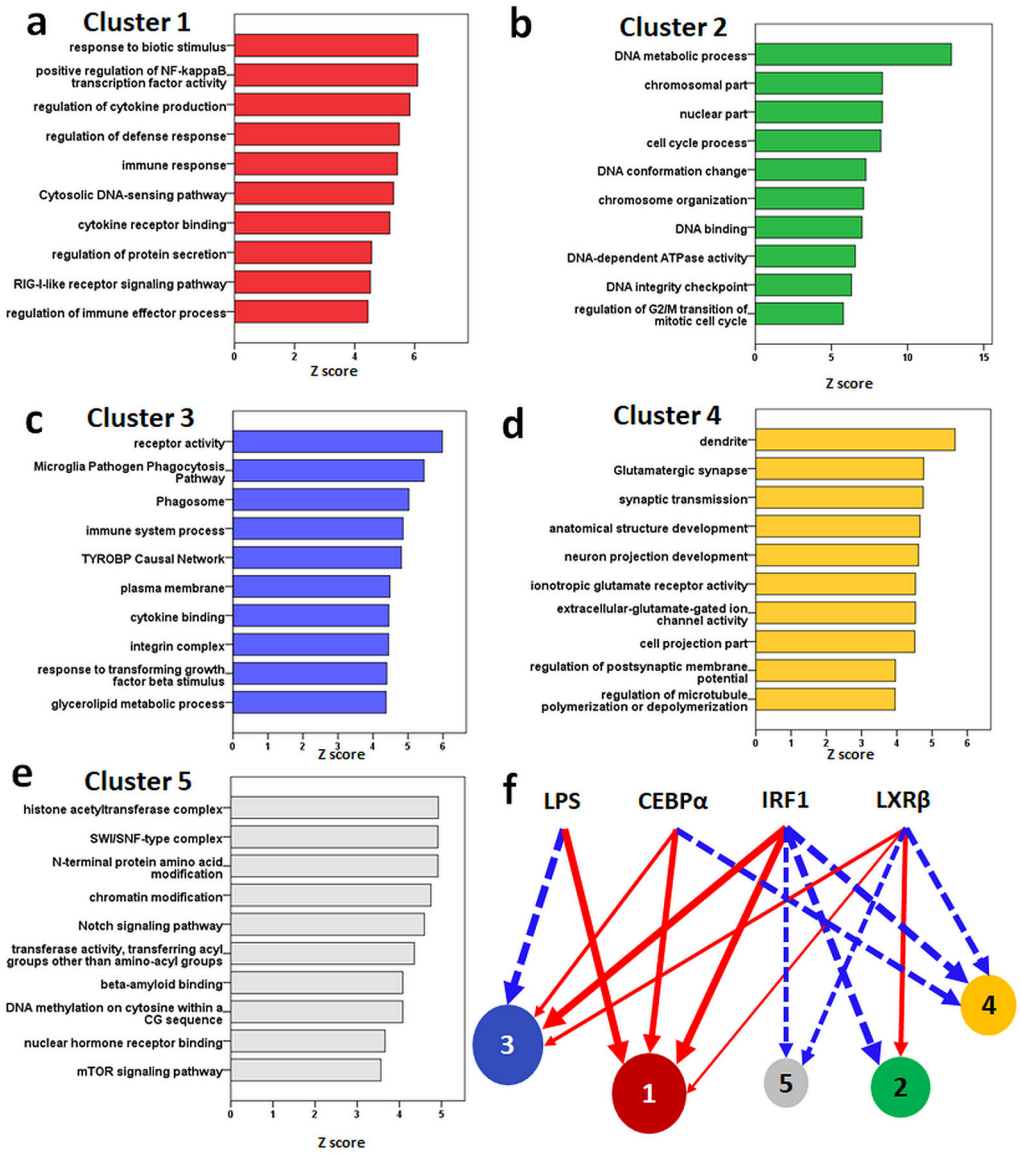

Figure 4. Gene ontology (GO) enrichment analysis of gene clusters and their regulation by IRF1, LXRβ and CEBPα.

(a-e) Top 10 GO terms enriched within each gene cluster (GO-Elite). Each cluster is color coded based on color schema used in Figure 3 (also see Supplemental Table S3 for complete lists of GO, KEGG and Wiki-pathway terms enriched in each gene cluster.) For GO analyses, input lists from each cluster were referenced to 662 genes included in the analysis. (f) Summary of regulation of each gene cluster by LPS, IRF1, LXRβ and CEBPα based on Nanostring analysis. Arrow color indicates direction of effect (Red: positive regulation, Blue: negative regulation). Arrow thickness indicates strength of association.

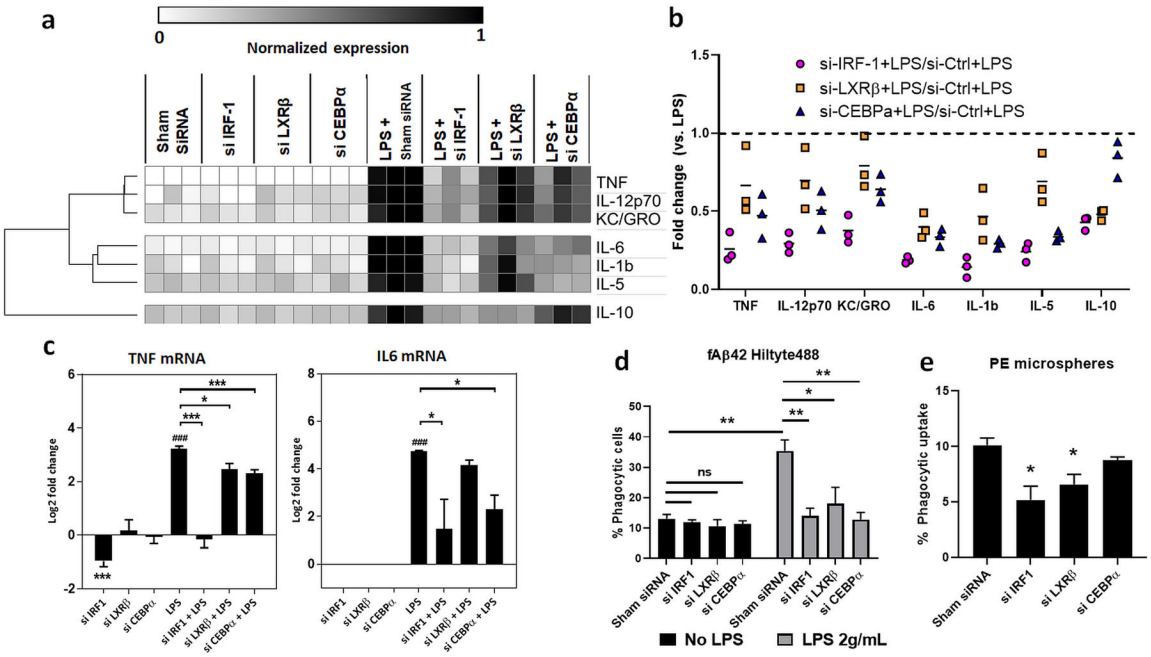

Figure 5. Regulation of pro-inflammatory cytokine production and phagocytosis by IRF1, LXRβ and CEBPα

(a) Hierarchical clustering analysis of pro-inflammatory cytokine data (MSD V-plex immunoassay) obtained from microglial culture supernatants after siRNA treatment and LPS (or sham) exposure.

(b) Fold change of pro-inflammatory cytokines (individual datapoints and mean shown) in siRNA + LPS treated microglia relative to sham siRNA + LPS treated microglia.

(c) qRT-PCR analyses of primary mouse microglia for Tnf and IL6 gene expression after siRNA exposure under resting and LPS-activated conditions. *p<0.05, ***p<0.005, ###P<0.005 compared to control siRNA.

(d-e) Comparison of *in-vitro* phagocytic capacity of primary microglia for fAβ42 Hiltyte488 (d) and polystyrene microspheres (e) following exposure to siRNAs against IRF1, LXRβ and CEBPα under resting and LPS-stimulated conditions (*p<0.05, **p<0.01, ***p<0.005, n=3 independently performed biological replicate experiments). Phagocytosis of fAβ42 was measured as proportion of fluorescent microglia using untreated microglia as negative controls. Phagocytic capacity for microspheres was measured as proportion of cells that take up >1 bead. For each sample, at least 2,000 live $CD45^+$ microglial events were captured.

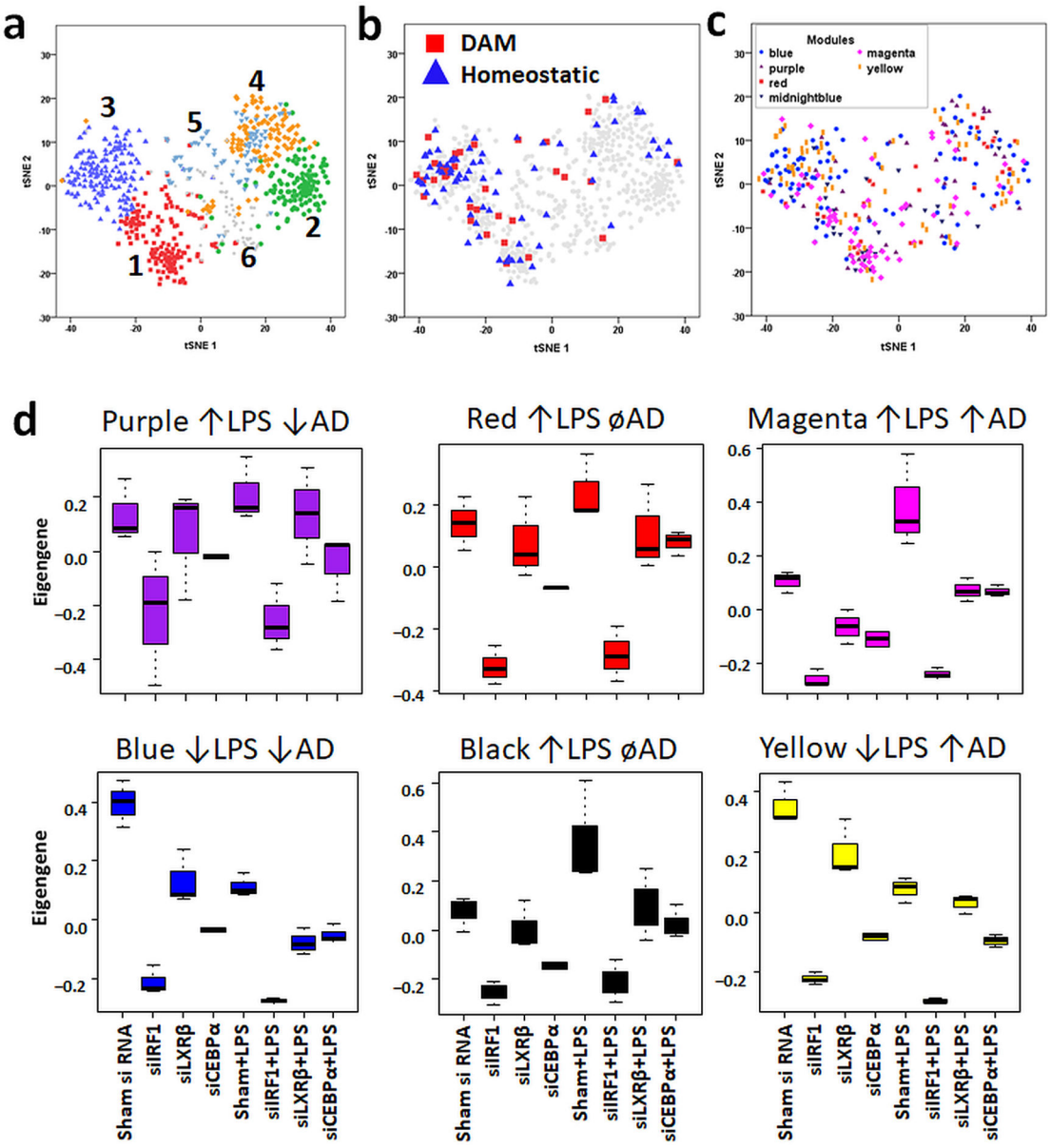

Figure 6. Regulation of homeostatic, pro-inflammatory DAM and anti-inflammatory DAM genes by IRF1, LXRβ and CEBPα

(a) 2D tSNE representation of Nanostring expression data identifies distinct clusters of co-expressed genes that agree with K-means clustering (color schema consistent with that used in Figure 3). Each dot in the tSNE plot represents a single gene.

(b) Enrichment of DAM and Homeostatic signature genes in Clusters 1 and 3. Grey dots represent genes not classified as DAM or Homeostatic. DAM and Homeostatic genes lists were obtained from a previously published single-cell RNAseq study of microglia (Keren-Shaul et al. 2017).

(c) Overlap between previously identified microglial co-expression modules identified by WGCNA (Rangaraju et al. 2018) with tSNE analysis of Nanostring expression data. Colors indicate microglial co-expression modules identified by WGCNA.

(d) Comparison of microglial co-expression module synthetic eigengene expression across various siRNA treatment conditions under resting and LPS-activated states. Six modules with >10 genes per module were identified (Homeostatic: Blue, Purple; LPS-upregulated but unrelated to AD: Red, Black; Pro-inflammatory DAM: Magenta; Anti-inflammatory DAM: Yellow). Hub genes (defined as top 20^{th} percentile of module membership or KMe) from a particular co-expression module that were present in the Nanostring gene set, were used for calculation of an aggregate "eigengene" to represent overall expression of the module across each experimental condition.

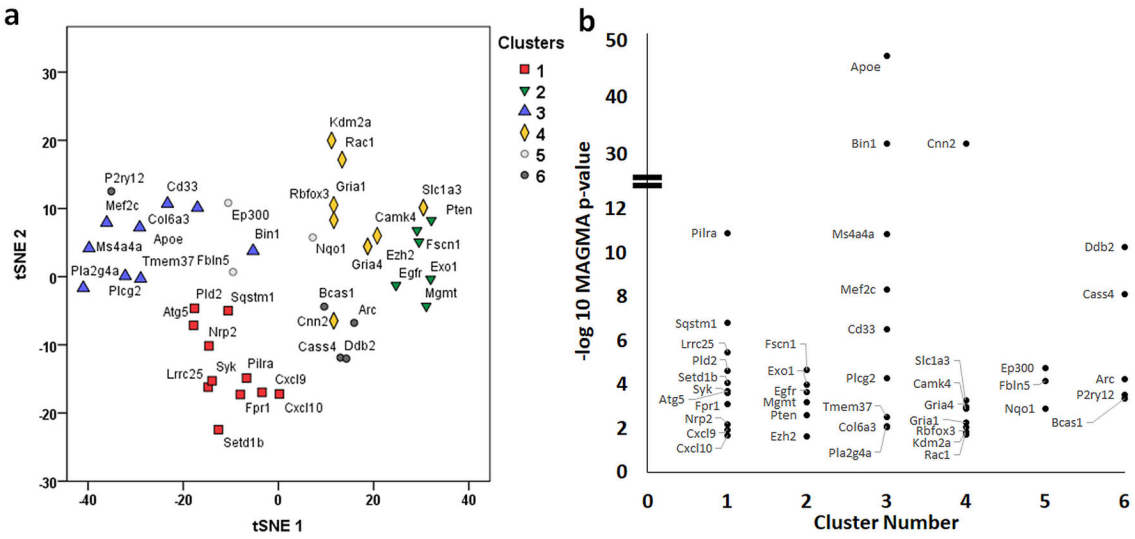

Figure 7. Regulation of AD-risk genes by IRF1, LXRβ and CEBPα.

(a) Distribution of 42 AD risk genes (identified by MAGMA of late-onset AD GWAS studies) across tSNE/K-means gene clusters. Of 1,234 AD risk genes identified by MAGMA, 42 AD risk genes were identified within 662 genes analyzed in the Nanostring panel. AD risk genes were not over-represented in any specific cluster of genes.

(b) Comparison of strength of genetic risk association (-log10 MAGMA p-value) of AD risk genes within in each cluster.

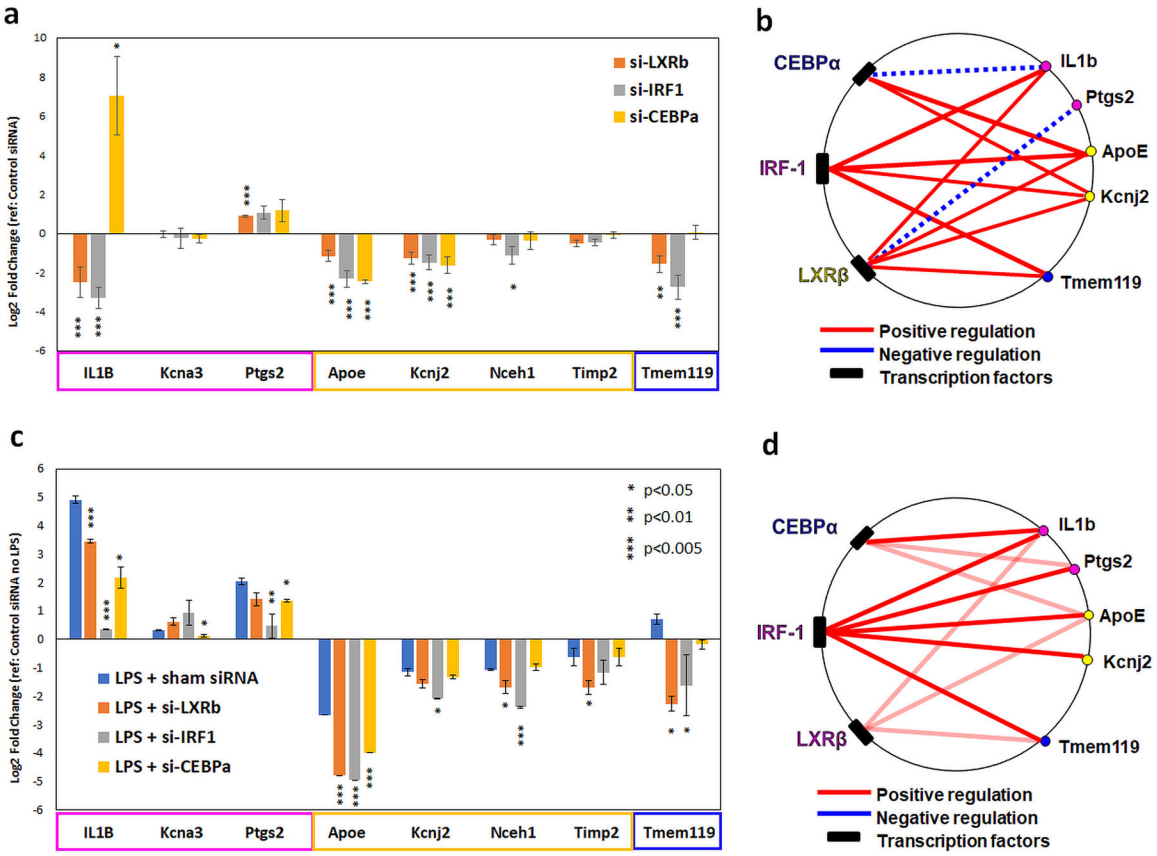

Figure 8. Validation of homeostatic and DAM gene regulation by IRF1, LXRβ and CEBPα.

(a) Results from qRT-PCR data comparing relative gene expression (log2 transformed relative expression) following siRNA exposure under resting conditions (n=3 independent biological replicates per condition. *p<0.05, **p<0.01, ***p<0.005). Error bars represent standard error of mean. X-axis: Magenta: Pro-inflammatory DAM genes; Yellow: Anti-inflammatory DAM genes; Blue: Homeostatic genes.

(b) Summary of regulation of homeostatic, pro- and anti-inflammatory DAM genes by TFs under resting conditions. Red arrow: positive regulation; Blue arrow: negative regulation; Arrow thickness indicates strength of association based on qRT-PCR studies.

(c) Results from qRT-PCR data comparing relative gene expression (log2 transformed relative expression) following siRNA exposure under LPS-activated conditions (n=3 independent biological replicates per condition. *p<0.05, **p<0.01, ***p<0.005).

(d) Summary of regulation of homeostatic, pro- and anti-inflammatory DAM genes by TFs under LPS-activated conditions. Red arrow: positive regulation; Blue arrow: negative regulation; Arrow thickness indicates strength of association based on qRT-PCR studies.

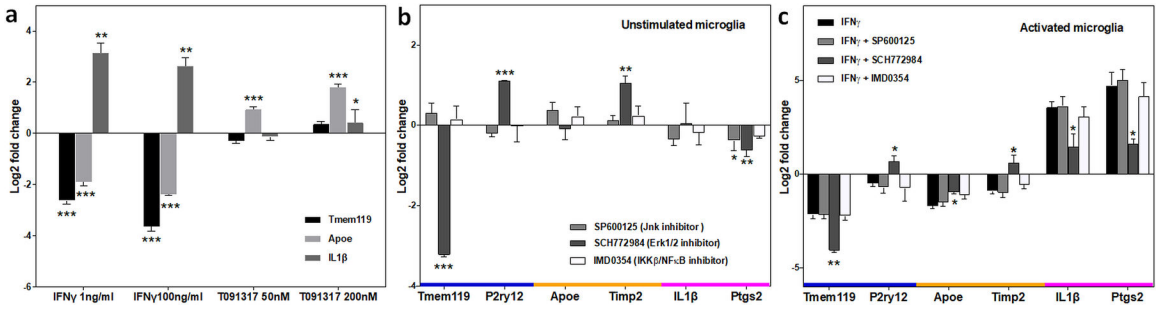

Figure 9. Regulation of homeostatic and DAM genes by IRF1 and LXRβ agonists and inhibitors of Erk, NFκB and Jnk signaling pathways

(a) Results from qRT-PCR studies comparing expression of Tmem119 (homeostatic), Apoe (DAM) and IL1b (pro-inflammatory DAM) genes following treatment of primary mouse microglia with IRF1 agonist IFNγ (1–100 mg/mL) and LXRβ agonist (T091317).

(b, c) Results from qRT-PCR studies comparing expression of homeostatic (Tmem119, P2ry12), anti-inflammatory DAM (Apoe and Timp2) and pro-inflammatory DAM (IL1b and Ptgs2) genes following treatment of primary mouse microglia with inhibitors of Erk1/2 signaling (SCH772984), Jnk signaling (SP600125) and NFκB signaling (IMD0354) under resting (b) and IFNγ-activated (1ng/mL) conditions (b). For all panels: All experiments were performed in independent biological triplicates; Error bars represent standard error of mean; *p<0.05, **p<0.01, ***p<0.005.

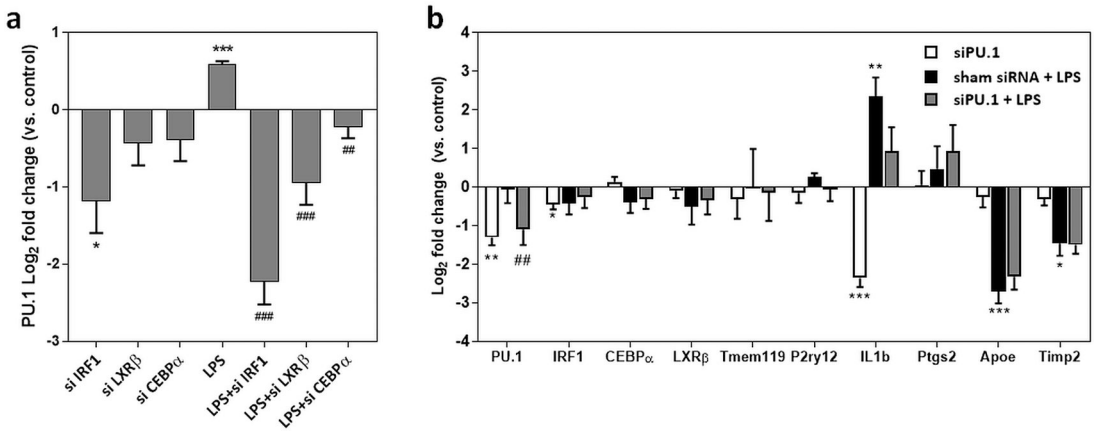

Figure 10. Reciprocal regulation between IRF1, LXRβ and PU.1 transcriptional factors in microglia.

(a) QRT-PCR experimental data comparing PU.1 mRNA expression (log2 transformed relative expression) after treatment of primary mouse microglia with siRNAs to silence IRF1, LXRβ and CEBPα in resting and LPS-activated conditions. (n=3 independent biological replicate experiments, error bars represent standard error of mean, *P<0.05, ***P<0.005, ## P < 0.01, ###P<0.001 compared to LPS-treated group).

(b) QRT-PCR experimental data comparing gene expression of TFs (PU.1, IRF1, LXRβ and CEBPα) as well as homeostatic (Tmem119, P2ry12), pro-inflammatory DAM (IL1b, Ptgs2) and anti-inflammatory DAM (Apoe, Timp2) genes after treatment of primary mouse microglia with PU.1 siRNA under resting and LPS-activated (2ng/mL) conditions. (Error bars represent standard error of mean, *P<0.05, **P < 0.01, ***P<0.005, ## P < 0.01 compared to LPS-treated group).

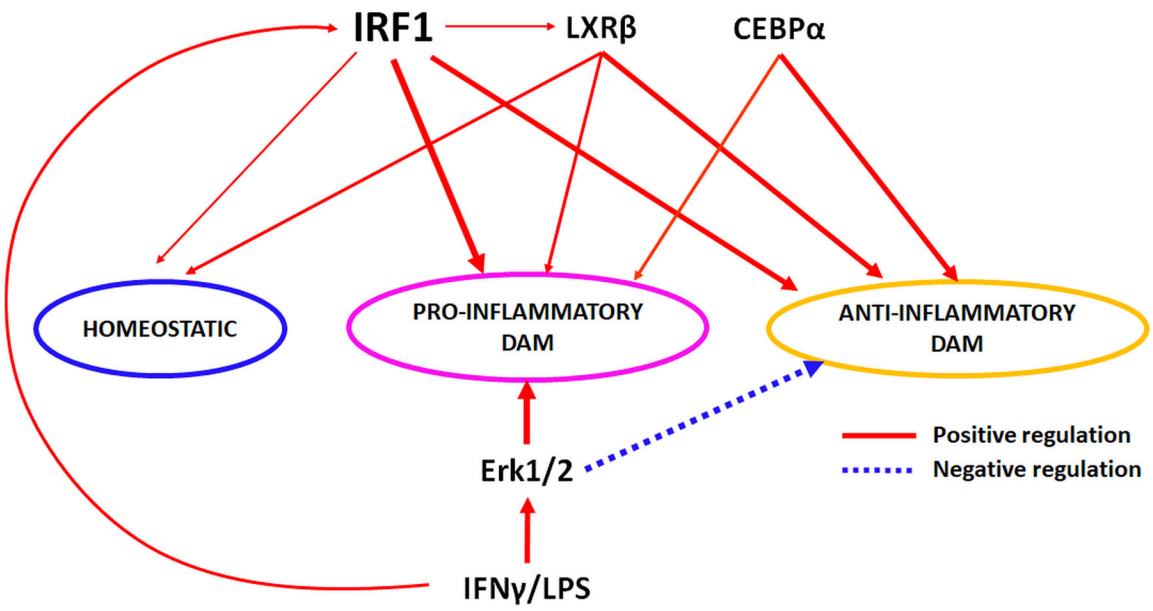

Figure 11. Transcriptional framework of homeostatic and DAM gene regulation in microglia.

A cohesive model of regulation of homeostatic and pro- and anti-inflammatory genes by TFs IRF1, LXRβ and CEBPα as well as by Erk1/2 pathways in microglia. Colors of arrows represent direction of regulation (Red: positive control; Blue: negative control). Thickness of the lines indicates strength of regulation.